AD-A107 301 MASSACHUSETTS INST OF TECH CAMBRIDGE RESEARCH LAB OF--ETC F/G 20/5
COMMUNICATIONS: FIBER-COUPLED EXTERNAL CAVITY SEMICONDUCTOR LAS--ETC(U)
JUL 81 R H REDIKER
UNCLASSIFIED N00014-80-C-0941
NL

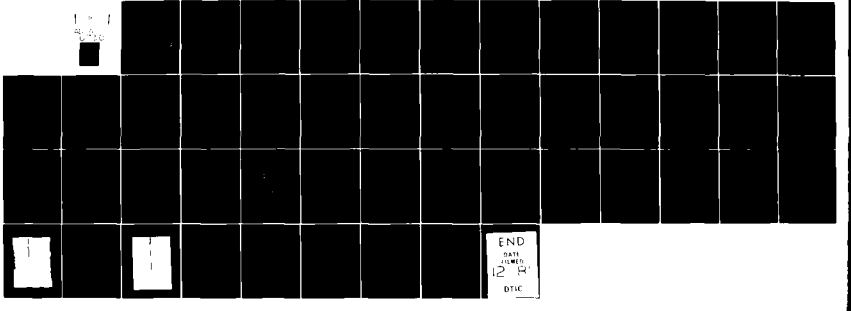

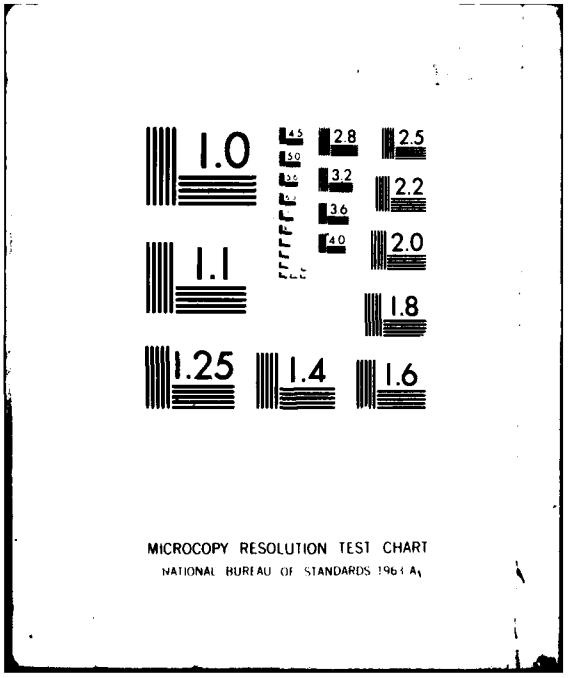
1.0
1.1
1.25
1.4
1.6
1.8
2.0
2.2
2.5
2.8
3.2
3.6
4.0
MICROCOPY RESOLUTION TEST CHART
NATIONAL BUREAU OF STANDARDS 1963 A

(12) LEVEL II

PROGRESS REPORT

Communications: Fiber-Coupled External Cavity Semiconductor Laser

Office of Naval Research
Contract N00014-80-C-0941

covering the period
1 July 1980 - 30 June 1981

Submitted by
Robert H. Rediker

July 1, 1981
~~September 10,~~ 1981

Massachusetts Institute of Technology
Research Laboratory of Electronics
Cambridge, Massachusetts 02139

UNCLASSIFIED

SECURITY CLASSIFICATION OF THIS PAGE (When Data Entered)

REPORT DOCUMENTATION PAGE		READ INSTRUCTIONS BEFORE COMPLETING FORM
1. REPORT NUMBER	2. GOVT ACCESSION NO.	3. RECIPIENT'S CATALOG NUMBER
4. TITLE (and Subtitle) (6) COMMUNICATIONS: FIBER-COUPLED EXTERNAL CAVITY SEMICONDUCTOR LASER,		5. TYPE OF REPORT & PERIOD COVERED (9) Annual Summary Report, 1 July 1980—30 June 1981,
		6. PERFORMING ORG. REPORT NUMBER
7. AUTHOR(s) (10) Robert H. Rediker		8. CONTRACT OR GRANT NUMBER(s) (15) N00014-80-C-0941
9. PERFORMING ORGANIZATION NAME AND ADDRESS Research Laboratory of Electronics Massachusetts Institute of Technology Cambridge, Massachusetts 02139		10. PROGRAM ELEMENT, PROJECT, TASK AREA & WORK UNIT NUMBERS NR 395-066
11. CONTROLLING OFFICE NAME AND ADDRESS Office of Naval Research Arlington, VA 22217		(11) 1 July 1981 13. NUMBER OF PAGES (12) 48
14. MONITORING AGENCY NAME & ADDRESS(if different from Controlling Office)		15. SECURITY CLASS. (of this report) Unclassified 15a. DECLASSIFICATION/DOWNGRADING SCHEDULE

16. DISTRIBUTION STATEMENT (of this Report)

Approved for public release; distribution unlimited

17. DISTRIBUTION STATEMENT (of the abstract entered in Block 20, if different from Report)

18. SUPPLEMENTARY NOTES

19. KEY WORDS (Continue on reverse side if necessary and identify by block number)

Laser
Semiconductor laser
Diode laser
Fiber-coupled external cavity
External cavity laser

20. ABSTRACT (Continue on reverse side if necessary and identify by block number)

The series combination of a semiconductor-diode gain element (a diode laser whose end facets have been antireflection coated) and an optical fiber has been placed inside an external cavity and the external cavity has lased in a single spectral line whose width was less than the 1.7×10^{-5}-nm resolution of the scanning Fabry-Perot interferometer used. When a grating in the Littrow configuration is used as one of the cavity end reflectors the spectral line can be tuned. Other elements such as a polarizer can also be placed inside the cavity to select

DD FORM 1 JAN 73 1473 EDITION OF 1 NOV 65 IS OBSOLETE

304650

UNCLASSIFIED

SECURITY CLASSIFICATION OF THIS PAGE (When Data Entered)

20. ABSTRACT

a desired mode of operation. The addition of elements inside the external cavity (including the optical fiber) introduces loss which increases both the threshold current for laser operation and the ratio of power at the gain element facet to cavity output power. With optimized design the long mean life of the semiconductor laser can be maintained by reducing the output power per gain element by less than 33 percent. In terms of the overall goal of this program, The Fiber-Coupled External Cavity Semiconductor Laser, the results obtained are extremely encouraging.

Abstract

The series combination of a semiconductor-diode gain element (a diode laser whose end facets have been antireflection coated) and an optical fiber has been placed inside an external cavity and the external cavity has lased in a single spectral line whose width was less than the 1.7×10^{-5}-nm resolution of the scanning Fabry-Perot interferometer used. When a grating in the Littrow configuration is used as one of the cavity end reflectors the spectral line can be tuned. Other elements such as a polarizer can also be placed inside the cavity to select a desired mode of operation. The addition of elements inside the external cavity (including the optical fiber) introduces loss which increases both the threshold current for laser operation and the ratio of power at the gain element facet to cavity output power. With optimized design the long mean life of the semiconductor laser can be maintained by reducing the output power per gain element by less than 33 percent. In terms of the overall goal of this program, The Fiber-Coupled External Cavity Semiconductor Laser, the results obtained are extremely encouraging.

I. Introduction

The thrust of this program is to demonstrate the feasibility of coupling semiconductor lasers in parallel using optical fibers and thus verify the concept of producing a laser system based on semiconductors with average power of the order of kilowatts. In this concept the optical fibers from the individual low-power semiconductor lasers are gathered together to act as a source for an external cavity with an appropriate spatial filter to assure that coherence is established over the entire optical-fiber bundle. The fibers are required so that the lasers can be used in subgroups "remote" from the cavity to reduce the power dissipation density.

The concept is attractive for application where high reliability is essential. Semiconductor lasers with estimated lifetimes of 10^6 hours have been reported.[1] Bell Telephone Laboratories are projecting lifetimes of 10^7 hours ($\sim$1000 years) for the lasers they will be using as sources in their fiber optics telecommunications net.[2] Another important consideration in the design of a high-power laser system for use in applications such as on space platforms, where prime power is at a premium, is the power efficiency of the laser systems. Semiconductor lasers have from the time of their invention shown promise for high efficiency. As a matter of fact, the original semiconductor lasers exhibited nearly 100 percent <u>differential quantum</u> efficiency when operated in a pulse mode at cryogenic temperatures.[3] As both understanding and the art have improved, power conversion efficiencies (wall-plug efficiencies) of 22 percent have been obtained for pulse operation at room temperature[4] and, recently, power conversion efficiencies of 35 percent have been obtained for cw operation at room temperature.[5]

The use of a spatial filter as proposed in this program to assure coherent output from an array of semiconductor lasers has been demonstrated.[6] Three lasers were forced into coherence by placing reflective strips where the maxima of the interference pattern would occur if the three lasers used were coherent. The optical peak power at room temperature was measured to be 5 W, three times the peak power of a single laser in the array. The use of an external cavity to control the wavelength at which a semiconductor-diode gain element (a semiconductor laser with its ends antireflection (AR) coated) in the cavity will lase has also been demonstrated. It has been shown[7] that, with an external

cavity, the laser radiation is produced in a single mode with no spectral or spatial hole-burning in the spontaneous spectrum. Thus the 35-nm spontaneous line is homogeneously broadened and the energy in this line is fed into the one mode. In these experiments the cw power in the laser line was 5 mW and its spectral width was less than 3.5 MHz or 8×10^{-6} nm.

Figure 1 is an artist's perspective illustrative of the configuration to be used in this program to demonstrate the feasibility of the Fiber-Coupled External Cavity Semiconductor Laser. One key element is the use of an optical fiber in series with the semiconductor-diode gain element in an external cavity. Since the electromagnetic mode of a semiconductor-diode gain element (laser) is TE and the electromagnetic mode of an optical fiber is HE, both different from the free-space mode, it was important to make certain that this combination of semiconductor-diode gain element and optical fiber performed appropriately in an external cavity. This report presents results which demonstrate that this combination does perform appropriately. As a matter of fact, the results presented in the subsequent sections are extremely encouraging in that they indicate that various "filters" can be placed inside the cavity in series with the semiconductor gain element/optical fiber combination to select the wavelength and the polarization of the fiber output. The results also indicate that multimode as well as single-mode fiber can be used.

There is interesting physics in the detailed electromagnetic mode propagation inside the external cavity through the semiconductor gain element, the optical fiber, and the various filter elements. In the work reported in this annual summary technical report we have only investigated this physics when it was felt that it was a means to the end of the feasibility demonstration of the Fiber-Coupled External Cavity Semiconductor Laser.

II. Experimental Apparatus

In this section we describe the experimental apparatus used in the compatibility study of the diode gain element and optical fiber when they are placed in series inside of an external cavity. Figure 2 illustrates the placement of optical components in the external cavity. Not shown is the Super-Invar four-bar structure that supports and aligns the separate components. The use of this Super-Invar structure is essential to obtain the stable monochromatic output required.[7] The figure includes all the components employed in various experimental arrangements used in this compatibility study to obtain the results presented in the next section. The individual experimental arrangements using subsets of these components are shown in the next section when the data corresponding to the arrangement are presented. Results are also presented in the next section for preliminary experiments not involving a fiber. The components used in this preliminary experiment are described at the end of this section.

As shown in Fig. 2, either a plane mirror or a grating (in the Littrow configuration) is used as the reflecting element at the left end of the external cavity. When the plane mirror is used it also serves as the output coupler. In most cases, a 40 percent reflectivity mirror is used. For the collimated beam normally incident on the plane mirror, the radiation is returned to its source. This does not provide for frequency selectivity other than that of the Fabry-Perot resonances of the entire external cavity. When instead of the mirror the grating is used in the Littrow configuration, it returns a narrow-band first-order beam collinear with the incident beam. The grating is effectively misaligned for all but this selected wavelength. The grating used has a ruling frequency of 1200 lines/mm and is blazed to return 90 percent of the incident beam intensity into the first order. Diffraction into the zero order of the grating provides output coupling. For either choice of end reflector, mirror or grating, the optic is held in a two-axis gimbal mount. Piezoelectric elements allow for fine-tuning the alignment. The gimbal mount is fixed to a plate through which the cavity structure's Super-Invar rods pass.

Proceeding to the right in the cavity, the next component is a collimating lens. This is a three-element lens system, AR coated for 820 nm on all internal glass-air interfaces. It has a 50-mm aperture and a 50-mm focal length. The lens is mounted directly into a plate through which the rods of the structure pass. The lens has no angular or transverse degrees of freedom. Only the position of the lens along the bars may be changed.

In the center of the cavity is the semiconductor-diode gain element. It is a (AlGa)As double-heterostructure diode laser obtained from Bell Telephone Laboratories. It is gain-guided in the dimension parallel to the plane of the junction and index-guided in the perpendicular dimension. When operated as a laser, it had a threshold of ∿100 mA with a peak emission wavelength of ∿820 nm. After the laser was received, it was sent to Design Optics, Sunnyvale, California to be AR coated on both facets. This reduced the reflectivity from 32 percent per facet to less than 0.5 percent from 810 nm to 840 nm. The diode chip is bonded to the top of a 2.5-cm-long copper stud. This stud is held in a specially designed x-y micropositioner machined from Invar. The positioner is mounted to two bars of the four-bar structure.

Continuing to refer to Fig. 2, to the right of the gain element is a cylindrical lens which compensates for the astigmatism inherent in the gain-guided/index-guided semiconductor-diode gain element. The purpose of the correction is to improve mode matching to the optical fiber. For a diode laser from the same batch as the diode gain element used, we measured a far-field divergence in the plane parallel to the junction plane (parallel direction) of 7 degrees full angle at half power (FAHP) and 22 degrees FAHP in the perpendicular direction. The cylindrical lens is oriented so as to reduce the divergence of the diode emission in the perpendicular direction while not changing the divergence in the parallel direction. The cylindrical lens is a drawn quartz fiber of 40 μm diameter, and is cemented to a miniature four-axis positioner which is mounted on the same stage as the diode. The lens is adjusted to obtain a far-field pattern that is roughly circular. The separation of the lens from the diode is on the order of the diameter of the lens.

The next element in the cavity is a graded-index (GRIN) rod lens used to change the now circular beam from diverging to converging. The index profile of the lens is parabolic, and light rays in such a medium will travel sinusoidal paths, oscillating back and forth across the optical axis. For the particular lens material used, the pitch of this oscillation is 21.9 mm. The lens is 0.25 pitch long, which is equivalent to a conventional spherical thin lens (of appropriate focal length), with a focal length of free space before and after the thin lens. The use of the graded-index lens is attractive from the standpoint of size (2-mm diameter, ∿5.5 mm long, ∿2-mm focal length) and light-gathering power (f/.96, or .46 NA). The lens is held in an arm attached to an x-y-z

micropositioner mounted on two bars of the four-bar structure. Alignment in the horizontal and vertical directions is aided by the use piezoelectrics on the x and y axes of the positioner. The axial (z-axis) position of the lens is optimized at the same time as the axial position of the optical fiber, to be described next.

Two types of optical fiber have been used in this study. The first fiber, Corning 4834 is single-mode with a 9 μm-diameter core. The fiber end faces were prepared by cleaving. The fibers were 14 cm long. In an attempt to prevent temperature fluctuations and stresses from affecting the fiber, and thereby the operation of the external cavity, the fiber was effectively placed at the center of a 2.36 cm-diameter Invar rod. In fact, a 1.18-cm-deep slot was machined for the 13-cm length of the rod and then a V-groove machined at the rod center. The fiber was laid in the V-groove and a piece of Invar designed to fit the slot, but with a foam bottom, was then placed in and completely occupied the slot. The ends of the fibers were waxed into 3-cm-long stainless steel needles (hollow tubes) to give rigidity and the V-groove made deeper at the ends to accommodate them. The preparation of the fibers required great care (e.g., the fibers were "threaded" into the hollow tubes before cleaving so no damage would occur to the cleaved end faces). Only very short (0.5 cm) ends of the fibers protrude from the end of the Invar rod. The Invar rod, along with the fiber, is positioned by an x-y-z micropositioner fixed to two rods of the four-bar Super-Invar structure.

Because of the importance of the state of polarization in the spatially-filtered multiple gain-element fiber-coupled external-cavity laser, such as shown in Fig. 1, it is important to investigate the operation of the series combination of a single semiconductor-diode gain element and optical fiber in the presence of a polarization-selective element. The next-to-last element in Fig. 2 is a polarizer. The objective of the polarizer is to preserve a constant state of polarization at the output of the fiber in the external cavity laser. The polarizer is the infrared type film mounted on a rotary stage. It is the only element not connected to the four-bar structure. Instead, the polarizer is supported from a post in the optical table next to the four-bar structure.

The last element in the external cavity laser is a spherical mirror. It has a 7.5-cm radius of curvature, centered on the output end of the optical fiber.

The mirror is coated for maximum reflectivity, and so cannot serve as an output coupler. The mirror is held in a two-axis gimbal mount, with fine adjustment of tilt accomplished by piezoelectric activated positioners. The gimbal mount is fixed to a plate through which the four rods of the cavity structure pass.

The light path in the external cavity is as follows. Light emitted from the left side of the AR coated laser diode is collimated by the spherical lens onto the plane mirror (or grating). The reflected (or first-order-diffracted) beam is reimaged onto the diode facet by the spherical lens. The emission from the right side of the diode passes through the cylindrical lens, the graded-index rod lens and into the fiber (single-mode or multimode). A polarizer, when present, filters the output of the fiber. The spherical mirror reflects and converges the diverging light, sending it back through the polarizer, and into the fiber. The emission of the fiber end nearest the diode is then focused into the diode by the action of the graded-index rod lens and the cylindrical lens.

Prior to the compatibility study of the semiconductor-diode gain element and optical fiber when they are placed in series inside of an external cavity, preliminary experiments were performed similar to those reported by Fleming and Mooradian[7] using a semiconductor-diode laser and then a semiconductor-diode gain element (a laser with its facets antireflection coated) inside an external cavity. The experimental arrangement in this case was that of reference 7. In this case a collimating lens is used on each side of a centrally located semiconductor gain element. As before, one side has a plane mirror or grating. The other side has a plane mirror. It should be pointed out that experimental apparatus described above and the experimental arrangements used in this report are built on the foundation of the arrangement used in reference 7.

Figure 3 shows the optical layout of those experiments to be described in the next section in which the plane mirror was used as the reflector at the left end of the cavity. Figure 4 shows the optical layout when the grating in the Littrow configuration is used instead of the plane mirror. These figures also illustrate the top view of the external cavity of Fig. 2. The four-bar Super-Invar structure on which the cavity components are mounted is also shown diagrammatically in Figs. 3 and 4. The diagnostics consist of a back-biased EG&G type SGD-440 photodiode for taking light output (lux)-current curves, and a Spex Model 1400-11 3/4 meter spectrometer or a Tropel Model 240-2 Scanning Fabry-Perot Spectrum Analyzer for measuring spectra. The resolution of the spectrometer was 0.05 nm and that of the Scanning Fabry-Perot 1.7×10^{-5} nm.

III. Experimental Results

A. Stimulated Emission (Lasing) Spectra

The experiments on the fiber-coupled external cavity laser were all done with the same semiconductor-diode gain element (diode laser whose end facets were antireflection (AR) coated). To obtain the spectra typical of a similar non-AR coated diode laser, another diode laser was chosen from the same batch obtained from Bell Telephone Laboratories (originally none of the batch were AR coated). The diode laser which was AR coated had a measured threshold current of 97 mA before coating. The diode laser whose spectrum is shown in Fig. 5 had a measured threshold current of 98 mA. The spectrum of Fig. 5 was obtained for a diode current of 99.3 mA. One can count 20 modes within the full-width-half-maximum of the envelope of lasing modes. The total number of lasing modes is more than three times this number. The mean wavelength is 828 nm and the interval between modes is 0.22 nm, consistent with a diode length of 350 μm.

When the diode of Fig. 5 was placed in an external cavity consisting of two lenses, a grating in the Littrow configuration, and a 40 percent reflectivity plane mirror as illustrated in the inset of Fig. 6, the spectrum shown in Fig. 6 resulted. The diode current was 98.1 mA, which is the current regime for which the diode, when not in the cavity, is superradiant. Superradiance as defined here occurs just above threshold where the light output (lux)-current curves start to depart from linearity but where laser oscillation has not yet occurred. Output was taken through the 40 percent reflectivity plane mirror. Because of the 32 percent reflectivity diode facets, the diode formed a subcavity within the larger external cavity. For this reason, the grating tuning was critical. When the grating was tuned into resonance with one of the diode modes, the increased feedback caused the selected mode to lase. In Fig. 6, this occurs at 829.1 nm. On either side of the laser line, one can see in the figure, at much lower intensity, modes due to the subcavity of the diode laser and its reflecting facets. The mode spacing is the same as in Fig. 5. For the conditions of Fig. 6, the measured power leaving the external cavity through the 40 percent reflectivity plane mirror was approximately 2 mW. At higher diode currents, the diode subcavity lased, no longer requiring the additional feedback of the external cavity, and the spectrum, accordingly, was no longer dominated by a single mode and looked more like the spectrum of Fig. 5.

The diode laser was removed from the external cavity and replaced by a semiconductor gain element whose end facets had been AR coated. The threshold current for this external cavity illustrated in the inset of Fig. 7 was measured to be 144 mA when the grating was tuned for minimum threshold current (which corresponds to maximum stimulated gain in diode gain element). The output consists of a single spectral line. As reported in Ref. 7 this single-spectral-line output can be tuned by the grating. The spectral line which is shown in Fig. 7 displays the tunability of the external cavity laser by illustrating the single-line laser emission when it is tuned to 816.7 nm. To obtain this spectral line the diode current had to be increased (to 178.1 mA for Fig. 7) because the threshold current increases away from the gain maximum at about 825 nm. Note in Fig. 7 the absence of spectral features indicative of reflections at the end facets of the semiconductor diode. These spectral features which are characteristic of the diode subcavity are still evident in the spontaneous emission, as will be discussed in section C below, and in the stimulated spectrum if the spectrometer sensitivity is increased by orders of magnitude over that used to obtain the data presented in Fig. 7. The laser output at 816.7 nm is single-mode to within the 0.05-nm resolution of the spectrometer.

After the preliminary experiments whose results are described above were concluded, the external cavity was altered for the compatibility study of the diode gain element and optical fiber when they are placed in series inside of the cavity. The left half of the external cavity (the collimating lens and the grating used in the Littrow configuration) remained unchanged. The components used in this configuration were discussed in depth in Section II. Output coupling was taken from the zero-order emission of the grating used in the Littrow configuration. The experimental arrangement in which the single-mode fiber was used is illustrated in the inset in Fig. 8. This figure also shows a typical spectrum. Single-mode emission was obtained at 823.1 nm. The diode current for this spectrum was 170 mA. Because of the losses in the additional optics, the threshold of this configuration was higher than that corresponding to the experimental arrangement of Fig. 7.

In the next experiment to be reported the grating was replaced with a 40 percent reflectivity mirror. The experimental arrangement is illustrated in the inset in Fig. 9. The spectrum in this figure was recorded with the diode current above the threshold current of 151 mA. The emission occurs between 824.3 nm and 824.4 nm, and was not single-mode over the duration of the

scan, recorded at 2 nm/min. However, since the external cavity was not thermally or acoustically shielded, it was not expected that the emission wavelength would remain temporally stable. In subsequent experiments reported below with the multimode fiber, the thermal and acoustic shielding of the cavity was improved and single-mode operation achieved, clearly indicating that it also could be achieved with the single-mode fiber. It should be pointed out that in the experiment neither the fiber ends nor the cylindrical lens were antireflection coated. (Concurrent with these experiments jigs were built and techniques developed to evaporate antireflection coatings of MgF_2 on the ends of the fibers prepared as described in Section II. In future experiments nonastigmatic diode lasers will be used, vitiating the need for the cylindrical lens.)

The next experiment to be described was performed to determine whether a multimode could be used to replace the single-mode fiber used in the external cavity for which the results have just been described. It was not a priori evident that such an external cavity, inside which a diode gain element which by itself can operate in many longitudinal modes is in series with a fiber which can also operate in a variety of modes, would be a viable laser. In fact, the results presented below indicate that it is. Several of these results are of interest. The coupling efficiency for radiation from the semiconductor gain element into the multimode fiber (as if it were to be used for fiber communication) was measured to be $\sim$70 percent while the similar coupling efficiency into the single-mode fiber was less than 20 percent. The threshold for lasing indicates, as will be described in section B below, that when the external cavity is lasing, the effective coupling efficiency of the radiation from the gain element into the multimode fiber is much less than 70 percent. This result is expected because the 70 percent efficiency is for coupling into many modes of the multimode fiber while, as determined experimentally from the laser spectrum, only a selected mode(s) of the fiber can participate in the laser action of the external cavity. This explanation can be restated in terms of the experimental arrangement shown in the inset of Fig. 10(a) by pointing out that the requirement that the laser mode(s) from the fiber output be "efficiently" reflected back into the fiber by the spherical mirror of the external cavity limits the number of fiber modes that can participate in lasing.

The threshold current for the experimental arrangement of Fig. 10(a) was 149 mA and a spectrum recorded at 170 mA of diode current is shown in the figure.

The spectrum shows a single line at 824.1 nm. A Fabry-Perot scan of the spectral line is shown in Fig. 10(b). The top trace in this figure shows the entire 1500 MHz free spectral range of this scanning interferometer, illustrating that there is but a single line and this free range corresponds to 14.2 msec of sweep (time between repeat of line). The bottom trace is a time expansion of the intensified gate around the right-hand line. The FWHM of the line is indistinguishable from the 7.5 MHz (1.7×10^{-5} nm) instrument resolution.

A polarizer was introduced to the cavity to verify that the external-cavity laser will operate successfully with a polarization-selective element. In Fig. 11(a) we show a typical spectrum recorded at 180 mA diode current for this configuration. A single spectral line was obtained at 829.8 nm, and the Fabry-Perot scan in Fig. 11(b) confirms that this was single-mode emission and also has a linewidth less than 1.7×10^{-5} nm. The threshold current was 167 mA. The polarizer was aligned parallel to the diode gain element polarization. We should remark that the polarizer is a lossy element even for this preferred polarization, and this insertion loss is in part responsible for the increase in threshold current. The particular polarizer had extremely high rejection when cross-polarized. It is clear that we can trade off less rejection of the cross-polarization for more transmission of the preferred polarization, resulting in a lowered threshold current and otherwise identical operation. This is characteristic of devices with homogeneously broadened gain elements, where if one mode of operation (a particular polarization, in this case) is given a reasonable advantage over other modes, the preferred mode will dominate to the exclusion of those other modes.

The temporal stability of the results presented above was also investigated. In particular, it was considered important to make sure that the measurements reported were <u>not</u> averages of fluctuations and that there was no spiking, short pulses or any other such phenomena in the output of the external cavity laser. With the Spex spectrometer tuned to the laser wavelength, the spectrometer photomultiplier output was measured for the diode gain element/multimode fiber configuration illustrated in the inset of Fig. 10(a), also for the configuration with the polarizer in place as illustrated in the inset in Fig. 11(a). To the 1-MHz bandwidth of the photomultiplier circuit there were no fluctuations, spikes, etc. for either configuration. Also, the output was stable for a period of the order of many minutes, the drift being very small considering the thermal variations expected. The output from the external cavity itself was measured,

using a TI avalanche photodiode in an appropriate circuit, to the bandwidth of 225 MHz of the Tektronix R7844 oscilloscope with the type 7A16 preamplifier at its full bandwidth. No fluctuations or spiking were seen for either configuration from baseband to the 225-MHz bandwidth. A note of caution needs to be mentioned. The elements in the external cavity need to be properly aligned. With incorrect alignment a large variety of temporal variations can be produced. This explains many results of others (published and unpublished) showing these variations both for a cavity consisting of the series combination of a semiconductor diode laser and a multimode fiber and for a semiconductor diode laser inside an external cavity. Our results were particularly gratifying for the configuration with the polarizer in place, as they showed that there was no fluctuation in the polarization of the output from the multimode fiber when it was used inside the external cavity.

B. Threshold Behavior

In this section we develop a simple model of the external cavity laser and find values of the losses in the laser consistent with measured threshold currents. The gain constant g in the active region of the diode gain element can be related in the regions of interest to the diode current I by

$$g = \beta(\eta_i I/\ell sd - J_o), \tag{1}$$

where η_i is the internal quantum efficiency, ℓ is the length of the diode, s is the width of the current distribution passing through the active region, d is the thickness of the active region, and β and J_o are constants.

The radiation inside the diode is not completely confined to the active region. A fraction Γ of the energy is inside the active region, and a fraction $1-\Gamma$ is outside, in the cladding layers. The distributed gain constant is therefore Γg. There is also a total internal distributed loss constant α related to the various loss mechanisms in the diode.

The external cavity laser model is shown in Fig. 12. A gain element, having the gain and loss constants of the diode gain element, is at the center. Its length is ℓ. There are absorbers with transmissions T_1 and T_2 to either side of the gain element. The reflectors at the ends have reflectivities R_1 and R_2. The threshold gain g_t must then satisfy the following condition

$$R_1R_2T_1^2T_2^2 \exp[2(\Gamma g_t-\alpha)\ell] = 1. \tag{2}$$

Solving the above equation for g_t and using Eq. 1 to obtain the threshold current, we find

$$I_t = \frac{\ell sd}{\eta_i}\left[\frac{\alpha - (1/\ell)\ln\sqrt{R_1R_2T_1^2T_2^2}}{\beta\Gamma} + J_o\right]. \tag{3}$$

In relating this equation to the experiments, it is useful to invert the equation and solve for $\sqrt{R_1R_2T_1^2T_2^2}$. For two resonators characterized by I_t, R_o,R_2,T_o,T_2 and I_t',R_1',R_2',T_1',T_2', we can relate the change in cavity parameters to the change in threshold as follows:

$$\exp\left[\frac{I_t' - I_t}{(sd/n_i\beta\Gamma)}\right] = \sqrt{\frac{R_1R_2T_1^2T_2^2}{R_1'R_2'T_1'^2T_2'^2}} \qquad (4)$$

As the reference cavity we will use the diode laser before its facets were antireflection (AR) coated. For this diode laser $R_1' = R_2' = 0.32$, $T_1' = T_2' = 1$, and $I_t' = 97$ mA. In the external cavity the known values of the end reflectors will be used and T_1 and/or T_2 will be determined from the experimental values of the threshold current using Eq. 4. (The threshold current is defined here consistent with accepted practice as the extrapolation of the stimulated emission-current curve to zero light output.)

In order to obtain values of T_1 and/or T_2 from Eq. 4, the factor $(sd/n_i\beta\Gamma)$ had to be determined. By rearranging Eq. 1, one obtains

$$\Gamma g\ell = \left(\frac{sd}{n_i\beta\Gamma}\right)^{-1} I + J_o\beta\Gamma\ell \qquad (5)$$

so that by determining g as a function of I one can obtain the desired factor. An approximate value for $(sd/n_i\beta\Gamma)$ was obtained experimentally as follows. The diode gain element was effectively removed from the external cavity. The spontaneous emission power leaving one side of the diode was measured for a particular diode current. Then a portion of the emission from the other side of the diode was re-injected into the gain element. Again the power output from the first side of the diode was measured, this power now including the emission injected into the other side and amplified by the gain element. By repeating the procedure at other currents one can obtain, as detailed in the Appendix, $\Gamma g\ell$ as a function of I, and thereby obtain, using Eq. 5, $(sd/n_i\beta\Gamma)$. This value which is a weighted average over the spontaneous emission yields a value of $(sd/n_i\beta\Gamma)$ of 19.8 mA. This number is used below to determine T_1 and/or T_2.

It must be pointed out that the values of T_1 and T_2 which will be given are the geometric mean of the transmission in the forward and backward directions of the component inserted in the cavity. (The transmissions in the two directions may be very different; e.g., there is less loss in going from the active region of the diode gain element to beyond a collimating lens than in going through the collimating lens back into the active region of the diode

gain element.) The transmission includes the collection efficiency of the component, and the efficiency with which the component re-injects the radiation into the active beam, as well as the efficiency with which the radiation is transmitted through the component.

The light output (lux)-current curves for the various configurations are shown in Fig. 13. We will now determine the values of T_1 and T_2 of the components used in these configurations from the threshold currents corresponding to the respective configurations. It should be first pointed out that experiments using a grating in the Littrow configuration cannot be used to determine the values of T_1 and/or T_2. The grating may tune the diode gain element away from the peak of its stimulated gain. In this case, Eq. 4 is incorrect because the two cavities being compared have different gains.

We first consider the external cavity laser shown in the inset of Fig. 7 except with the grating replaced by a 98 percent reflecting plane mirror. It used a diode gain element, two collimating lenses, a 40 percent reflectivity plane mirror, and the 98 percent plane mirror. The threshold was 135 mA. Because, apart from the end reflectors, the cavity is symmetric, we should have $T_1 = T_2$. Using Eq. 4, with $R_1 = 0.4$, $R_2 = 0.9$, $I_t = 143$ mA, we find $T_1 = T_2 = 0.27$.

We next consider the external cavity configuration shown in the inset of Fig. 9. To the left of the diode the configuration is identical to that in the inset of Fig. 7, so the value for $T_1 = 0.27$ is applicable to the new configuration. To the right of the diode the new configuration contains a single-mode optical fiber. A cylindrical lens and a graded-index lens are used between the diode and fiber, and an ∿100 percent reflectivity mirror defines the end of the cavity. The threshold was 151 mA. Equation 4, with $R_1 = 0.4$, $R_2 = 1$, $T_1 = 0.27$, $I_t = 151$ mA, predicts a value of $T_2 = 0.12$. This is the mean transmission (forward and backward propagation) through the cylindrical lens/graded-index lens/single-mode fiber combination, including coupling efficiencies into the active region of the gain element and both ends of the fiber.

When the single-mode fiber was replaced by a multimode fiber of the same length (see inset of Fig. 10), the threshold dropped to $I_t = 149$ mA. All other optics were as before, so that $R_1 = 0.4$, $R_2 = 1$, $T_1 = 0.27$. Using these values, Eq. 4 predicts a value of $T_2 = 0.13$. While we stated above that T_2 (or T_1) is related to the collection efficiency of, and the transmission of radiation through,

the component one must be very careful in the use of these terms. The multimode fiber collects 70 percent of the radiation from the diode gain element and the single-mode fiber 18 percent but the value of T_2 for the multimode fiber is only about 1.1 times that for the single-mode fiber. The explanation, as mentioned in section A, is that only selected mode(s) of the multimode fiber can participate in the lasing of the external cavity, because only selected modes are reflected back into the fiber by the spherical mirror in appropriate phase and angle to participate in the laser emission.

C. Spontaneous Emission Spectra

When the external cavity laser is operated below threshold, features are seen in the spontaneous emission spectrum that can be related to subcavities of the laser. As stated earlier, the above-threshold spectrum of a particular external cavity configuration had exhibited no features indicative of the original diode laser that now served as the gain element. This was attributed to the successful application of AR coatings to the diode laser facets. However, we can find evidence of residual reflectivity on these and other optical surfaces by examining the spontaneous emission spectrum. When two aligned, sufficiently reflective, optical surfaces exist within the external cavity, Fabry-Perot-type resonances occur characteristic of this subcavity. It is important to identify, understand, and minimize these effects, since they can influence the operation of the external cavity and its tunability. Certainly, reducing the effects of subcavities is desirable, and it is important to identify them with this end in mind.

In Fig. 14 we show a below-threshold spectrum corresponding to an external cavity consisting of a single-mode fiber, a plane mirror, a spherical mirror, appropriate lenses, and the gain element. (An above-threshold spectrum for this configuration was shown in Fig. 9.) The first subcavity we identify is responsible for the 0.22-nm period substructure in the figure. After comparing this substructure to the mode spacing of a diode laser from the same batch of diodes as the gain element (Fig. 5), we can assume that both the laser mode spacing there and the spectral substructure here are due to the same cavity. (The spacing $\Delta\lambda$ = 0.22 nm is consistent with a Fabry-Perot etalon, 350 μm long, index of refraction n = 3.63, and dispersion $dn/d\lambda = -0.001\ nm^{-1}$, that is, the diode.)

The second subcavity we identify modulates the spontaneous emission spectrum with a substructure having a period much longer than the diode subcavity, approximately 3 nm. This corresponds to a subcavity bounded at one end by the facet of the diode facing the cylindrical lens and at the other end by the concave second surface of the lens. Light diverges from the gain element from a facet having some nonzero reflectivity (as evidenced by the substructure due to the diode subcavity). This light passes into the cylindrical lens through its convex first surface. Reflections from this surface diverge and are lost. As the light leaves the lens, some light is reflected from the concave second surface.

This light is convergent and couples back into the gain element. Thus the pertinent optical length is from the front facet of the diode gain element to the second surface of the cylindrical lens. The fused-quartz lens is 40 μm in diameter; it has a refractive index of 1.45. The spacing, $\Delta\lambda$ = 3 nm, is consistent with a 55 μm gap of air between the diode and lens as measured by the microscopic observations of this gap.

It is also possible to identify a substructure with a 0.04-nm periodicity. This substructure can be attributed to the graded-index lens, with length 55 mm and (on-axis) refractive index 1.6. The 0.04-nm substructure is barely visible for a combination of two reasons. First, the graded-index lens has been AR coated and second, the resolution of the spectrometer is 0.05 nm. Any substructure due to longer optical lengths, such as the 14-cm length of the optical fiber, would be far beyond the resolution limit of the spectrometer. It should be pointed out that the bump in the spontaneous emission curve near 824 nm is where the external cavity would lase, if the diode current were higher. The features shown in Fig. 13 are typical of the spontaneous emission spectra recorded in every configuration. While we cannot resolve any substructure related to reflections between the ends of the optical fiber, we have developed the jigging and the techniques necessary to AR coat the ends of the fiber, concurrently with performing the experiments reported here. Finally, the cylindrical lens, which was responsible for the most severe (highest contrast) modulation of the spontaneous spectra examined, was needed because we were using an astigmatic gain element. For further phases of our research program, Bell Laboratories has promised to supply us with nonastigmatic diodes, obviating the need for cylindrical lenses.

IV. Discussions and Conclusion

The feasibility of operating a semiconductor-diode gain element in series with an optical fiber inside an external cavity has been demonstrated. If a grating in the Littrow configuration is used instead of one of the end mirrors of the cavity, the single spectral line output of spectral width less than 1.7×10^{-5} nm of the cavity can be tuned. We have also shown that for the external cavity laser, the polarization of the output of the fiber into the cavity can be selected by simply using a polarizer at this output. This polarization selection and wavelength selection by the use of "filter elements" inside the cavity will aid in the realization of the Fiber-Coupled External Cavity Semiconductor Laser, which is the goal of this program. The insertion of lossy elements inside the cavity has the deleterious effects of decreasing the overall (wall-plug) efficiency mainly by increasing the threshold current, and of increasing the power density at the facets of the semiconductor gain element for a given cavity power output. The semiconductor diode lasers (the semiconductor-diode gain elements before they were AR coated) received from Bell Telephone Laboratories for this program were rated a 5-mW output per facet (7.4 mW incident on the facet from inside the semiconductor) on the basis that their lifetime (reliability) would be reduced by higher power output.[8] This facet erosion effect, unlike facet damage which occurs at over an order of magnitude higher output power, is not due to the electric field at the facet and no definitive statement can be made as to whether AR coating the diodes has any effect on facet erosion.[8] We will assume the 7.4 mW incident on the facet to produce 5 mW output for the diode laser causes the erosion irrespective of the surface reflectivity. The decrease in overall efficiency should not have any effect on reliability.

The amount of loss inserted into the cavity in the feasibility experiments described in this report is much larger than would be inserted in an operating system. While the coupling efficiency for the radiation from the semiconductor gain element into the single-mode fiber was 18 percent for the experiments reported here, coupling efficiencies larger than 50 percent have been reported by a number of workers in the field using more sophisticated optics.[9-11] The more sophisticated optics require manufacturing techniques that would be developed for a system. For example, in reference 11, the fibers are fabricated with

quadrangular pyramid-shaped hemielliptical ends – to produce these ends equipment developed to manufacture phonograph needles was used. The results reported above for the single-mode fiber experiments are, in fact, very encouraging. For the external cavity the single-mode fiber and associated optics gave an equivalent transmission T_2 (see Sec. III-B above) of 0.12. Since the coupling into the fiber from the laser was 0.18, the additional insertion loss in the lasing state including coupling to/from the end spherical mirror is quite reasonable considering that the experiments were designed to show feasibility and not optimized operation.

If one assumes that the Fiber-Coupled External Cavity Laser will have a configuration of the form of Fig. 1 with the back facet of the lasers coated for unity reflection, the front facets AR coated and the output mirror with 0.1 reflectivity, and referring now to Fig. 11, $T_1 = 1$ and $T_2 = 0.5$; then the output from the external cavity laser per semiconductor gain element will be 66 percent of the output from the diode laser before its facets were coated. Specifically, for the 5-mW output diode lasers used in the feasibility experiments reported above, and for the power incident on the facets of 7.4 mW, which maintains the long life (high reliability) of the diodes, the external cavity output per diode will be 3.3 mW.

In this section we have addressed the issue of maintaining the long mean life to failure (10^5-10^6 hours) of the semiconductor laser when used as a gain element in an external cavity laser. We have used as example the lasers used in the feasibility study reported here, where facet erosion is the failure mechanism. It should be made clear that other semiconductor laser types from other manufacturers (or the same manufacturer) have been built or may be built where facet erosion is not the limiting factor in reliability. For example, it has been reported[12] that the use of transparent (AlGa)As at the facets (the gain region in the semiconductor diode is surrounded in every direction by regions that are transparent to the radiation!) has reduced significantly the "mirror oxidation" and increased significantly the lifetime of the lasers.

In summary, we have demonstrated the feasibility of operating a semiconductor-diode gain element in series with an optical fiber inside an external cavity laser. In addition, the results we have obtained increases our confidence that the Fiber-Coupled External Cavity Semiconductor Laser feasibility experiment, the goal of this program, will be successful.

Acknowledgments

The work described in this report was performed using equipment at and partially supported by M.I.T. Lincoln Laboratory. This work will also be reported in part in M.I.T. Lincoln Laboratory technical reports. We thank A. Mooradian, D. Welford, and B. Feldman for advice and assistance. We also thank E.I. Gordon, R.W. Dixon, and R.L. Hartmann of Bell Telephone Laboratories for supplying us with the diode lasers and for extremely valuable discussions.

Participants in Research Reported

Robert H. Rediker	Adjunct Professor of Electrical Engineering
Robert P. Schloss	Graduate Student, Department of Electrical Engineering and Computer Science

Appendix

We describe here the method by which $(sd/\eta_i\beta\Gamma)$ was estimated for the semiconductor-diode gain element, where sd is the cross-sectional area of the diode active area, η_i is the internal quantum efficiency, β relates the gain of the active region to the diode current through Eq. 1, and Γ is the radiation confinement factor.

The diode gain element is first removed from the external cavity. While operating with current I we measured spontaneous emission power P leaving the front facet of the diode. The power exiting the rear of the diode is proportional to the power leaving the front. Let us call this power cP, where c is a constant (approximately 1, although this is not necessary). Now we insert optics behind the diode such that a fraction k of the light is re-injected into the diode gain element. The diode has gain g (for current I) and absorption α. The power now measured in front of the diode is $P + ckP \exp[(\Gamma g-\alpha)\ell]$. We repeat these two measurements for various currents. Figure A1 plots the power leaving the front facet of the diode versus current without (lower curve) and with (upper curve) a portion of the rear facet emission re-injected.

If we denote the fractional change of power, $\Delta P/P$ (upon re-injecting some rear-facet emission), by r, then we can write the following:

$$\ln r = \ln ck + \Gamma g\ell - \alpha\ell. \tag{A1}$$

We can relate r to the current I by using a modified version of Eq. 1 (see Section III-B):

$$\Gamma g\ell = \left(\frac{sd}{\eta_i\beta\Gamma}\right)^{-1} I - J_0\beta\Gamma\ell. \tag{A2}$$

Inserting this into Eq. A1, we find

$$\ln r = \left(\frac{sd}{\eta_i\beta\Gamma}\right)^{-1} I + [\ln ck - (\alpha+J_0\beta\Gamma)\ell], \tag{A3}$$

from which we predict a linear relationship between ln r and I whose slope is $(sd/\eta_i\beta\Gamma)^{-1}$. In Fig. A2 we plot the logarithmic fractional change ln r from Fig. A1, from 140 mA to 170 mA. Also indicated is the line that best fits the

data. The reciprocal slope of this line, 19.8 mA, is our approximation to $(sd/\eta_1 \beta\Gamma)$. It should be emphasized that this value represents a weighted average over the spontaneous emission and is being used as a good approximation for analyzing the onset of stimulated emission.

References

1. S. Nita, H. Namizaki, S. Tahamiya, and W. Susaki, "Single-Mode Junction-UP TJS Lasers with Estimated Lifetime of 10^6 Hours," IEEE J. Quant. Electron. 15, 1208 (1979).

2. E. I. Gordon, Bell Telephone Laboratories, private communication.

3. T. M. Quist, R. H. Rediker, R. J. Keyes, W. E. Krag, B. Lax, A. L. McWhorter, and H. J. Zeiger, "Semiconductor Maser of GaAs," Appl. Phys. Lett. 1, 91 (1962).

4. H. Kressel, H. F. Lockwood, and F. Z. Hawrylo, "Large-Optical-Cavity (AlGa)As-GaAs Heterojunction Laser Diode: Threshold and Efficiency," J. Appl. Phys. 43, 561 (1972).

5. N. Chinone, K. Sarto, R. Ito, K. Aiki, and N. Shige, "Highly Efficient (GaAl)As Buried Heterostructure Lasers with Buried Optical Guide," Appl. Phys. Lett. 35, 513 (1979).

6. E. M. Philipp-Rutz, "Spatially Coherent Radiation from an Array of GaAs Lasers," Appl. Phys. Lett. 26, 475 (1975).

7. M. W. Fleming and A. Mooradian, "Spectral Characteristics of External-Cavity-Controlled Semiconductor Lasers," IEEE J. Quant. Electron. 17, 44 (1981).

8. R. W. Dixon, Bell Telephone Laboratories, private communication.

9. M. Sarawatari and K. Nawata, "Semiconductor Laser to Single-Mode Fiber Coupler," Appl. Opt. 18, 1847 (1979).

10. J. Yamada, Y. Murakami, J. Sakai, and T. Kimura, "Characteristics of a Hemispherical Microlens for Coupling between a Semiconductor Laser and Single Mode Fiber," IEEE J. Quant. Electron. 16, 1067 (1980).

11. H. Sakaguchi, N. Seki, and S. Yamamoto, "High Efficiency Coupling from Laser Diodes into Single-Mode Fibers with Quadrangular Pyramid-Shaped Hemielliptical Ends," Tech. Digest of 1981 Conf. on Int. Optics and Optical Fiber Commun. (April 1981).

12. H. Yonezu, M. Ueno, T. Kamejima, and I. Hayashi, "An AlGaAs Window Structure Laser," IEEE J. Quant. Electron. 15, 775 (1979).

Figure Captions

Fig. 1. Fiber-coupled external cavity semiconductor high-power laser illustrating from left-to-right: the semiconductor-diode gain element whose left facet is coated for near unity reflectivity and whose right facet is antireflection coated (this element would be a semiconductor laser if its right facet were not antireflection coated); electro-optic element; focusing lens; spatial filter to assure coherence of wavefront across entire fiber bundle emitter (this spatial filter is illustrated as a stop); focusing lens to recollimate beam; and a partially reflecting mirror. The external cavity is bounded on the left by the reflecting facets of the semiconductor gain elements and on the right by the partially reflecting mirror.

Fig. 2. Experimental arrangement showing placement of components inside Super-Invar four-bar external cavity. The components are described in more detail in text. Actual experimental arrangements for specific experiments, in which subsets of these components are used, are shown in insets in the figures presenting experimental results.

Fig. 3. Optical layout of experiments in which a plane mirror was used as the reflector/output coupler at the left end of the cavity. Not all components are used all the time. External cavity laser components are shown in a top, cutaway view through the four-bar Super-Invar structure. The *labeled elements are: PM — plane mirror*; SL — spherical collimating lens; D — diode gain element; CL — cylindrical lens; GL — graded-index rod lens; F — optical fiber; P — polarizer; SM — spherical mirror.

Fig. 4. Optical layout of experiments in which a grating in the Littrow configuration was used as the reflector/output coupler at the left end of the cavity. The labeled elements are: LG — grating used in the Littrow configuration; SL — spherical collimating lens; D — diode gain element; CL — cylindrical lens; GL — graded-index rod lens; F — optical fiber; P — polarizer; SM — spherical mirror.

Fig. 5. Typical spectrum of a semiconductor laser diode received from Bell Telephone Laboratories. Another diode from the same batch was AR coated and used as the gain element in later experiments. Threshold current for the diode whose spectrum is illustrated is 98 mA. Operating current during the spectrum is 99.3 mA. The envelope of modes peaks at 828 nm with a full width at half power of 4 nm, and the modes themselves are spaced every 0.22 nm.

Fig. 6. Spectrum obtained when the laser diode from Fig. 5 was placed in a grating-tuned external cavity. The diode is positioned at the middle of the cavity (see inset). On either side of the diode are collimating lenses. End reflectors are a 40 percent reflectivity plane mirror and a diffraction grating used in the Littrow configuration. The diode laser is operating in its superradiant regime (see text). External cavity laser emission occurs at 829.1 nm.

Fig. 7. Stimulated emission spectrum obtained when the semiconductor diode gain element (AR coated laser diode) was placed in a grating-tuned external cavity. Operating current is 178.1 mA and laser emission occurs at 816.7 nm. When cavity is tuned by the grating for minimum threshold, laser emission occurs at approximately 825 nm.

Fig. 8. Stimulated emission spectrum obtained when a single-mode fiber is placed in series with the diode gain element inside a grating-tuned external cavity. A cylindrical lens and graded-index lens couple the diode and left end of the fiber. A spherical mirror, at whose center of curvature is the right end of the fiber, serves as one end reflector for the external cavity. Reflectivity is approximately unity. The reflector at the other end of the cavity is a grating used in the Littrow configuration. Diffraction efficiency into first order is approximately 90 percent. Output coupling is taken from the zero order. Operating current is 170 mA. Laser emission occurs at 823.1 nm.

Fig. 9. Stimulated emission spectrum obtained when the diode gain element and a 14-cm-long single-mode fiber are placed in an external cavity in which neither end reflector is frequency-selective. The grating from Fig. 8 was replaced by a 40 percent reflectivity plane mirror. Output coupling is taken through the mirror. Laser emission occurs between 824.3 nm and 824.4 nm.

Fig. 10(a). Stimulated emission spectrum obtained when the diode gain element and a 14-cm-long multimode fiber are placed in an external cavity in which neither end reflector is frequency-selective. A 40 percent reflectivity plane mirror and an approximately unity-reflectivity spherical mirror are used. Operating current is 170 mA. Laser emission occurs at 824.1 nm.

Fig. 10(b). Spectrum as measured by Fabry-Perot scanning interferometer. Top trace in this figure shows the entire 1500-MHz free spectral range of this scanning interferometer, illustrating that there is but a single line and this free range corresponds to 14.2 msec of sweep (time between repeat of line). Bottom trace is a time expansion of the intensified gate around the right-hand line. The FWHM of the line is indistinguishable from the 7.5 MHz (1.7×10^{-5} nm) instrument resolution.

Fig. 11(a). Stimulated emission spectrum obtained when the diode gain element, a 14-cm-long multimode fiber, and a polarizer are placed in an external cavity in which neither end reflector is frequency-selective. A 40 percent reflectivity plane mirror and an approximately unity-reflectivity spherical mirror are used. The polarizer is aligned parallel to the diode gain element polarization. Operating current is 180 mA. Laser emission occurs at 829.8 nm.

Fig. 11(b). Spectrum as measured by Fabry-Perot scanning interferometer. Top trace in this figure shows the entire 1500-MHz free spectral range of this scanning interferometer, illustrating that there is but a single line and this free range corresponds to 14.2 msec of sweep (time between repeat of line). Bottom trace is a time expansion of the intensified gate around the right-hand line. The FWHM of the line is indistinguishable from the 7.5 MHz (1.7×10^{-5} nm) instrument resolution.

Fig. 12. Single-ended power output P_o as a function of diode current, I, for various configurations.

(A) The diode laser which was later AR coated to become gain element for other curves. Threshold is 97 mA.

For curves (B)-(E) the gain element is at the center of an external cavity which is bounded at its left end by a 40 percent reflectivity plane mirror. The output power which is plotted in these curves is that measured through the mirror.

(B) AR coated gain element in cavity with collimating lenses and plane cavity mirrors. At right end of cavity the plane mirror has 98 percent reflectivity. Threshold is 135 mA.

(C) Multimode fiber in right half of cavity in series with gain element. At right end of cavity is an ∿100 percent reflectivity spherical mirror. Threshold is 149 mA.

(D) Single-mode fiber in right half of cavity in series with gain element. At right end of cavity is an ∿100 percent reflectivity spherical mirror. Threshold is 151 mA.

(E) Polarizer at the output of multimode fiber in right half of cavity in series with gain element: At right end of cavity is an ∿100 percent reflectivity spherical mirror. Threshold is 167 mA.

(F) Cavity spoiled by blocking reflector at right end of cavity.

Fig. 13. Simple model of external cavity laser used for analyzing threshold currents observed for various configurations. This is a "plane-wave" model, in contrast with the actual configuration. The (transverse-) modal nature of the external cavity laser elements are suppressed in drawing, but lumped into the loss elements T_1 and T_2. As required, these nonphysical elements will incorporate such factors as coupling from an optical fiber to the diode (and vice versa), coupling from a plane mirror to the diode through a collimating lens, and coupling from a spherical mirror to an optical fiber at its center of curvature. T_1 and T_2 also include neutral density attenuation and any other relevant losses in the cavity.

Fig. 14. Spontaneous emission spectrum of external cavity laser configuration consisting of diode gain element, 14-cm-long single-mode fiber, 40 percent R plane mirror, ∿100 percent R spherical mirror, and appropriate lenses. Resonances characteristic of subcavities are seen. These subcavities are discussed in text.

Fig. A1. Front-facet power output of diode gain element versus injection current. (A) With a portion of emission from the rear facet re-injected into the diode. (B) Without re-injection. From these curves one can extract the quantity $(sd/\eta_i \beta\Gamma)$, as discussed in text.

Fig. A2. Semilogarithmic plot of fractional change r in power, $\Delta P/P$, determined from curves A and B in Fig. A1. Only the interval from 140 mA to 170 mA is plotted. A least-squares fit to the data (assuming a linear relationship) is superimposed. The reciprocal slope of this line is the value of $(sd/\eta_i \beta\Gamma)$ used in Section III-B.

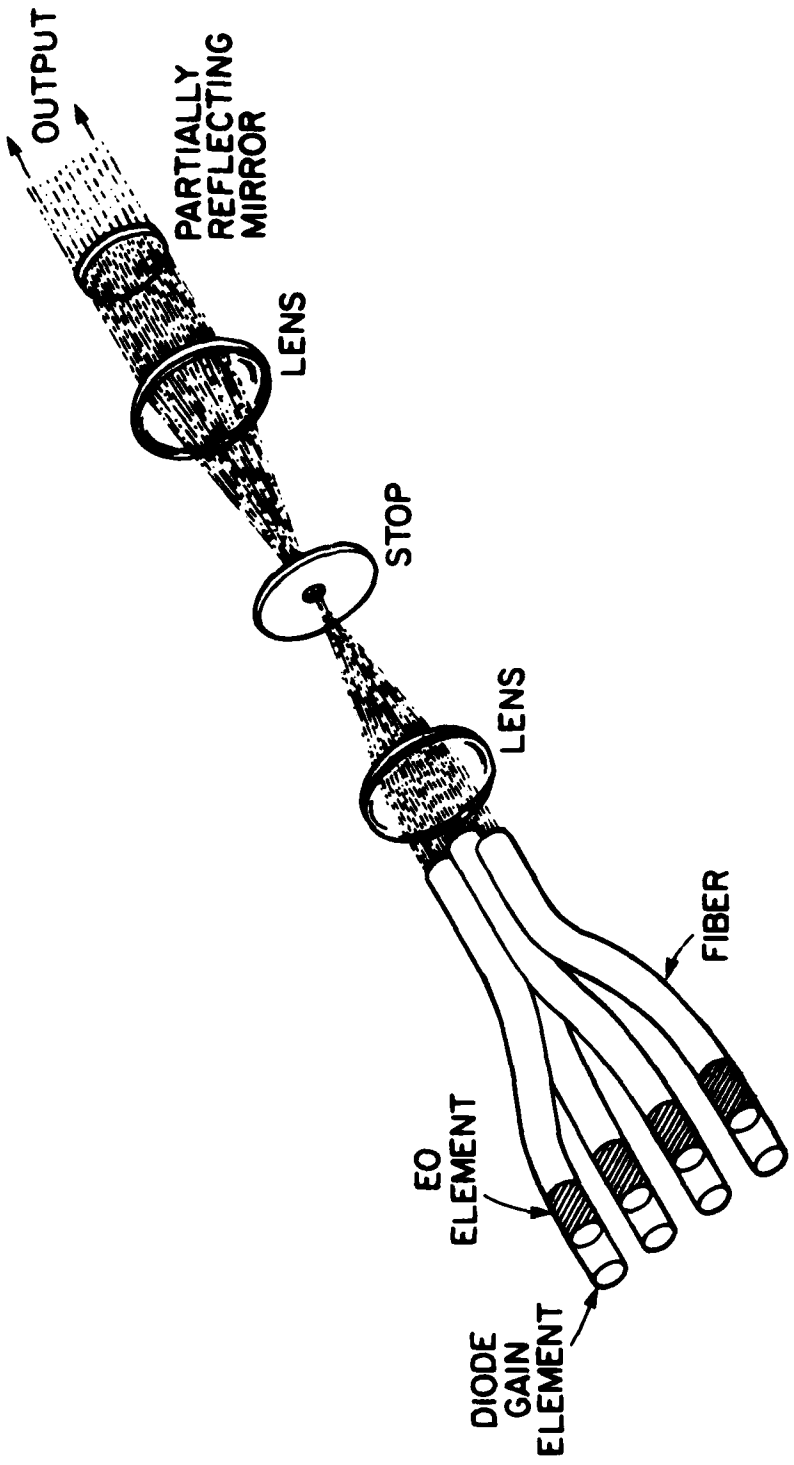
OUTPUT
PARTIALLY REFLECTING MIRROR
LENS
STOP
LENS
FIBER
EO ELEMENT
DIODE GAIN ELEMENT

Figure 1

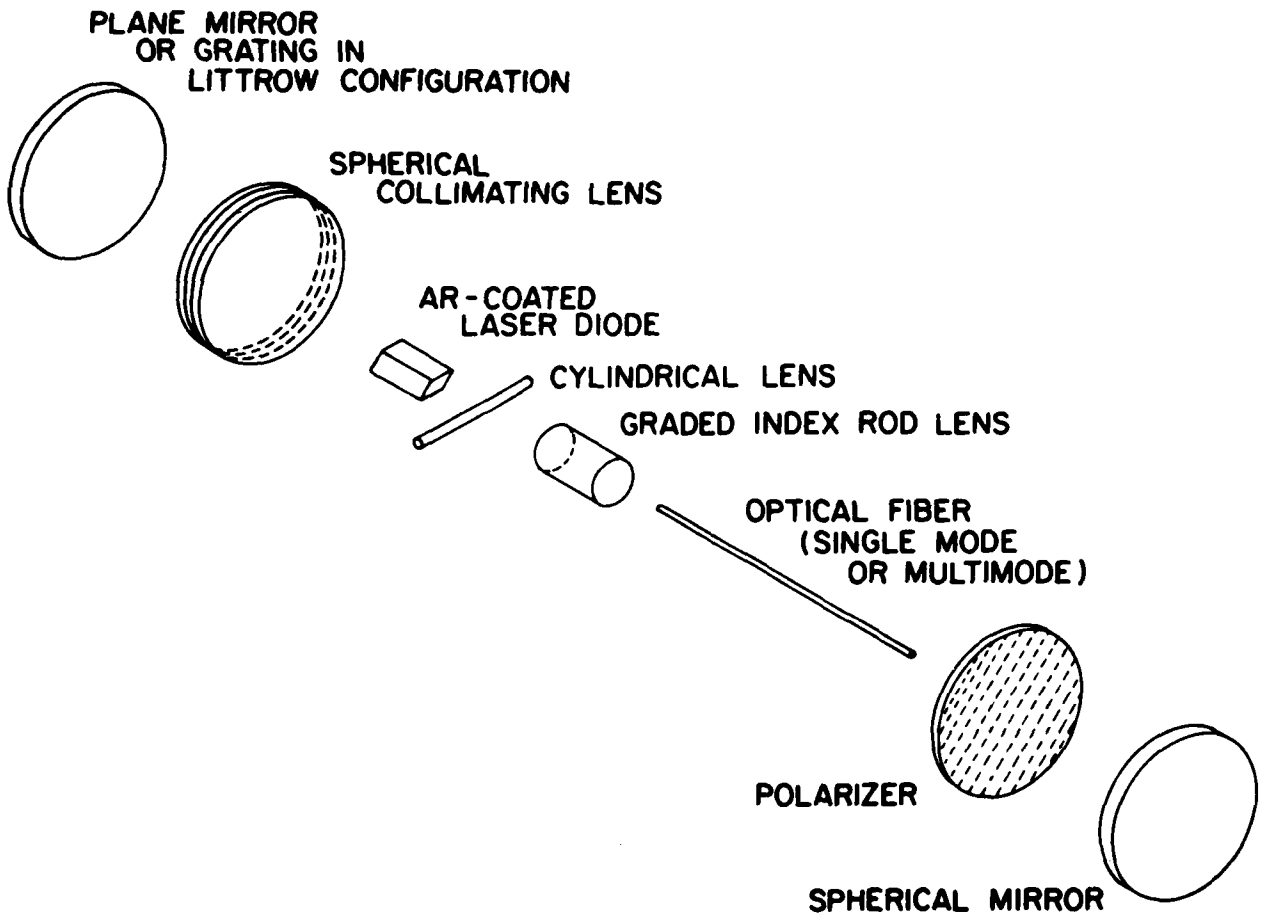
PLANE MIRROR
OR GRATING IN
LITTROW CONFIGURATION
SPHERICAL
COLLIMATING LENS
AR-COATED
LASER DIODE
CYLINDRICAL LENS
GRADED INDEX ROD LENS
OPTICAL FIBER
(SINGLE MODE
OR MULTIMODE)
POLARIZER
SPHERICAL MIRROR

Figure 2

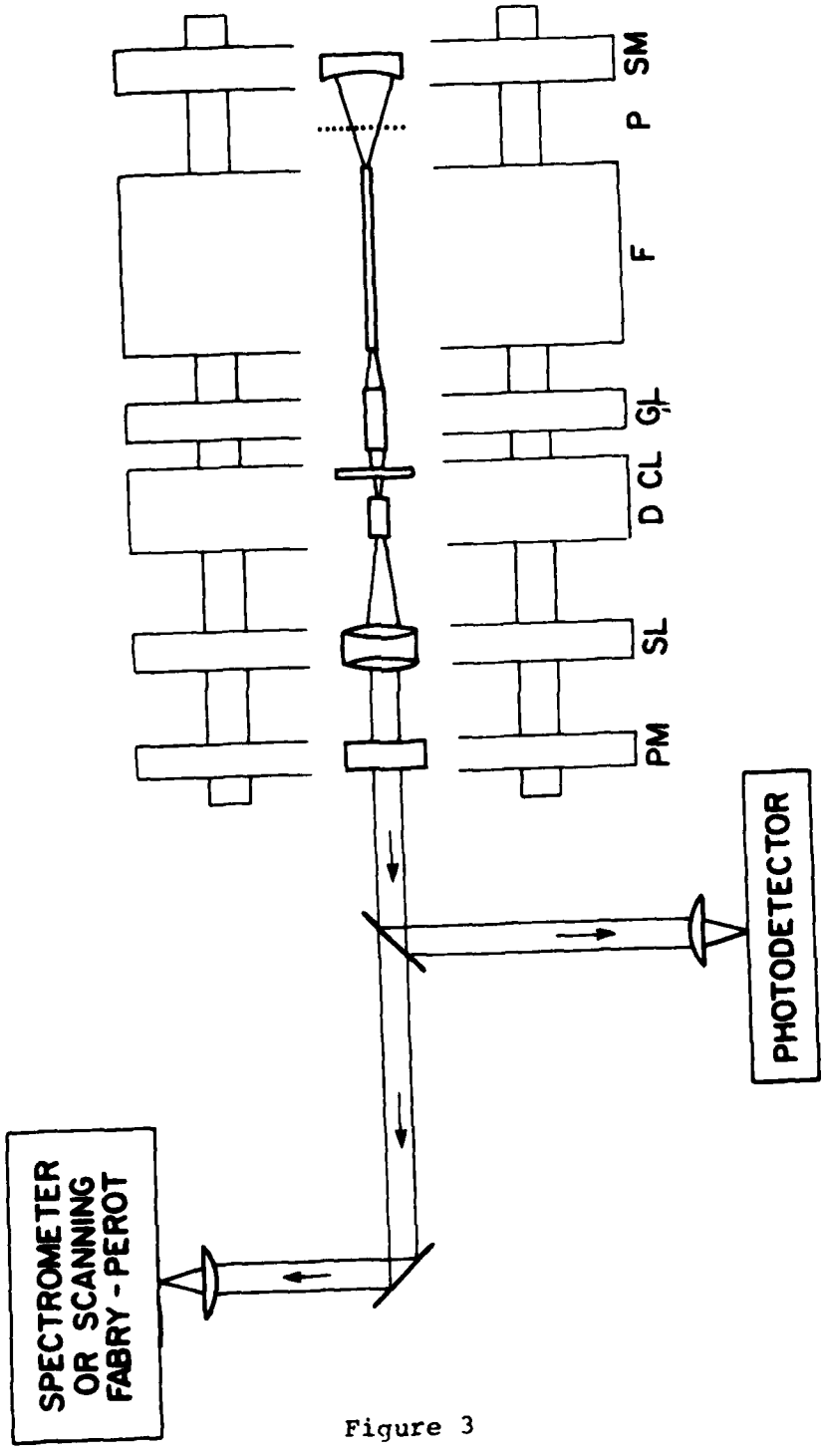
SM
P
F
GL
D CL
SL
PM
PHOTODETECTOR
SPECTROMETER
OR SCANNING
FABRY - PEROT

Figure 3

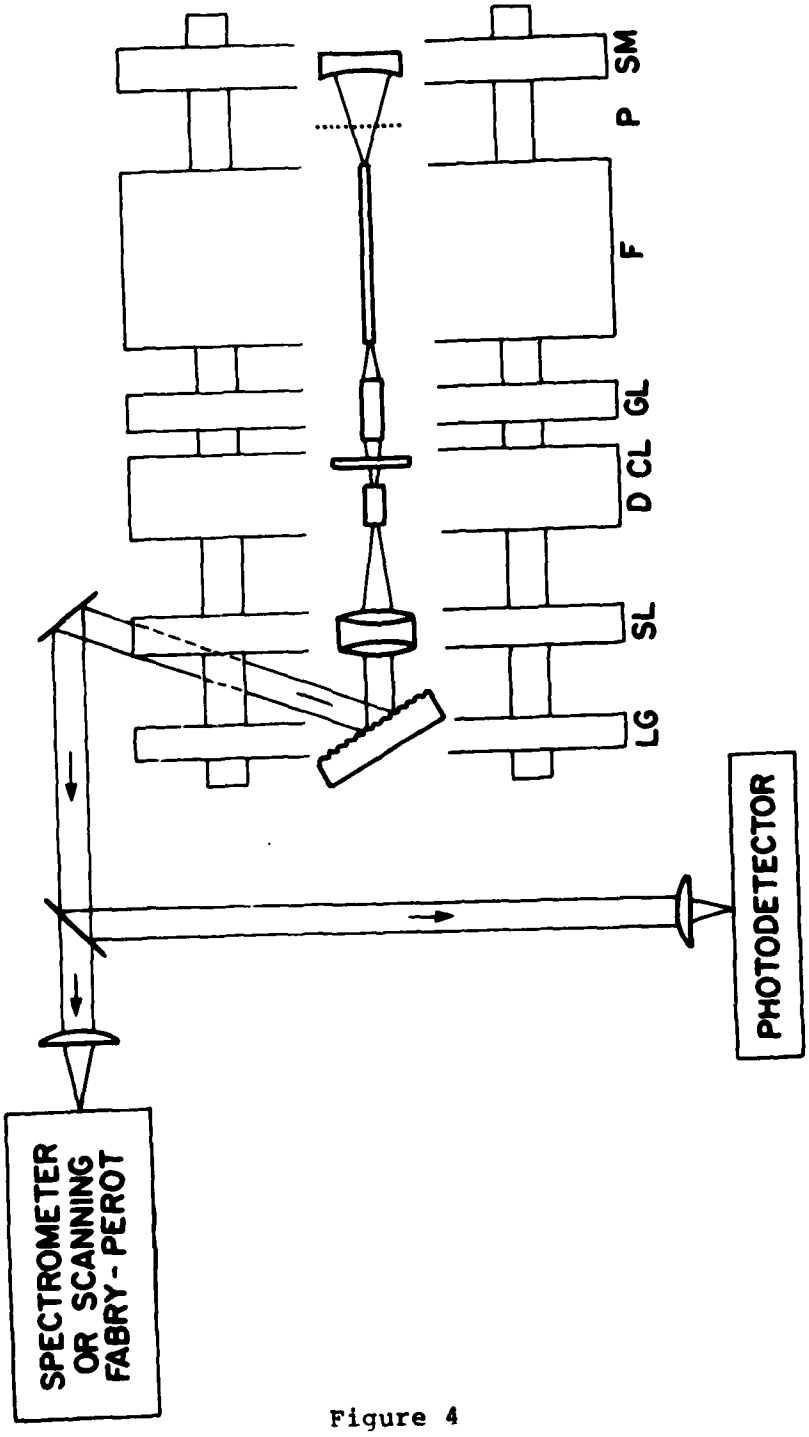
P SM
F
GL
D CL
SL
LG
PHOTODETECTOR
SPECTROMETER OR SCANNING FABRY-PEROT

Figure 4

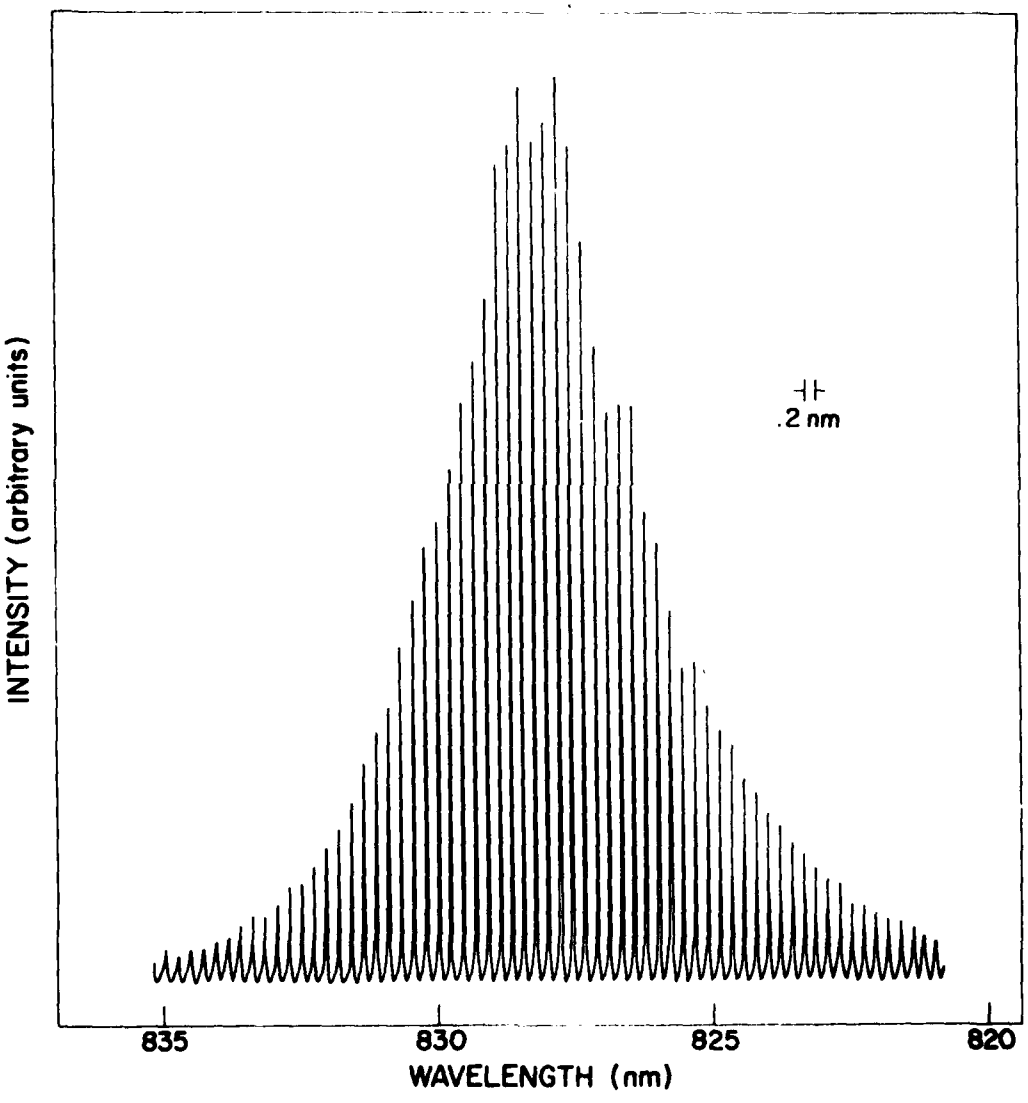
INTENSITY (arbitrary units)
.2 nm
835
830
825
820
WAVELENGTH (nm)

Figure 5

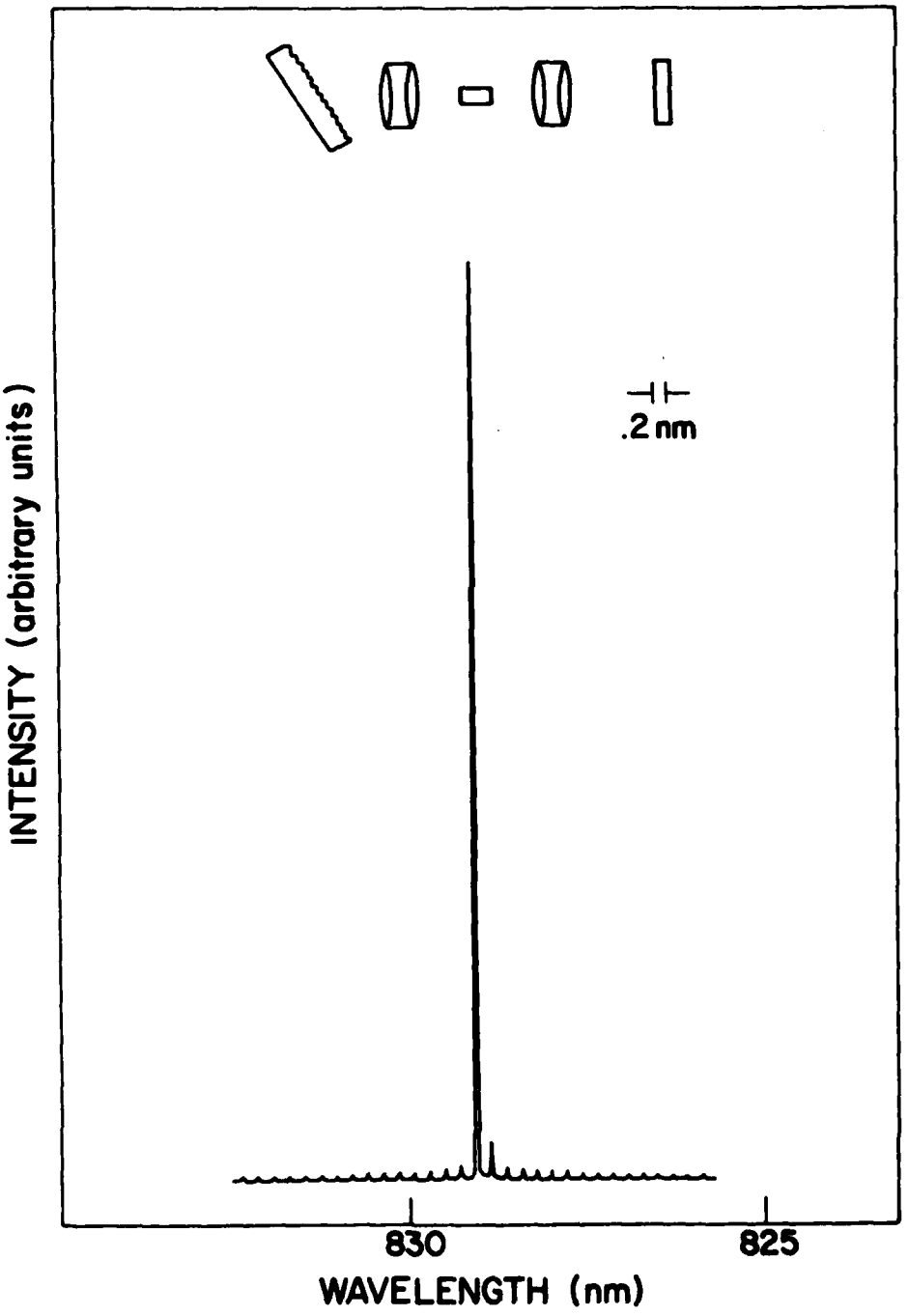

Figure 6

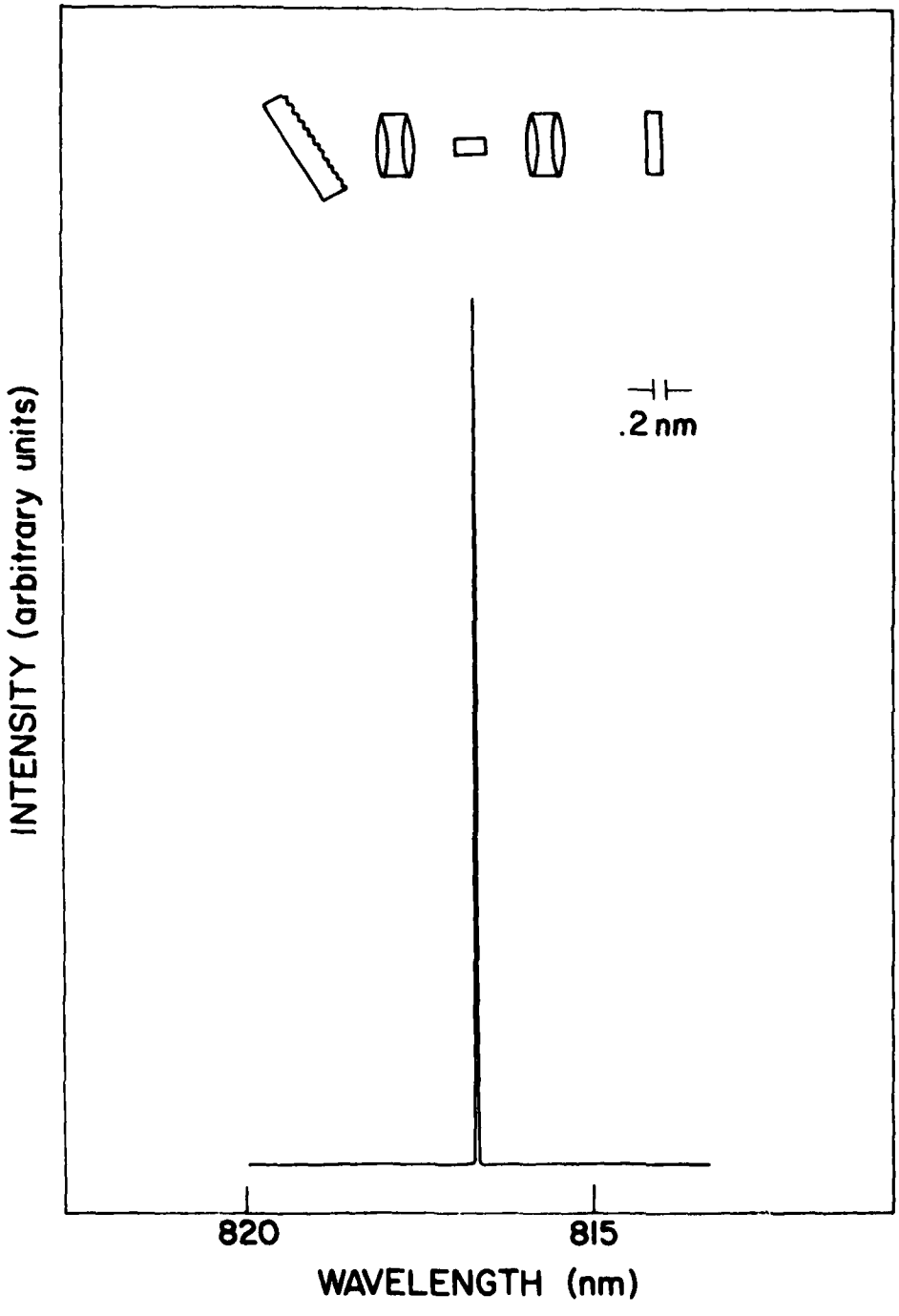

Figure 7

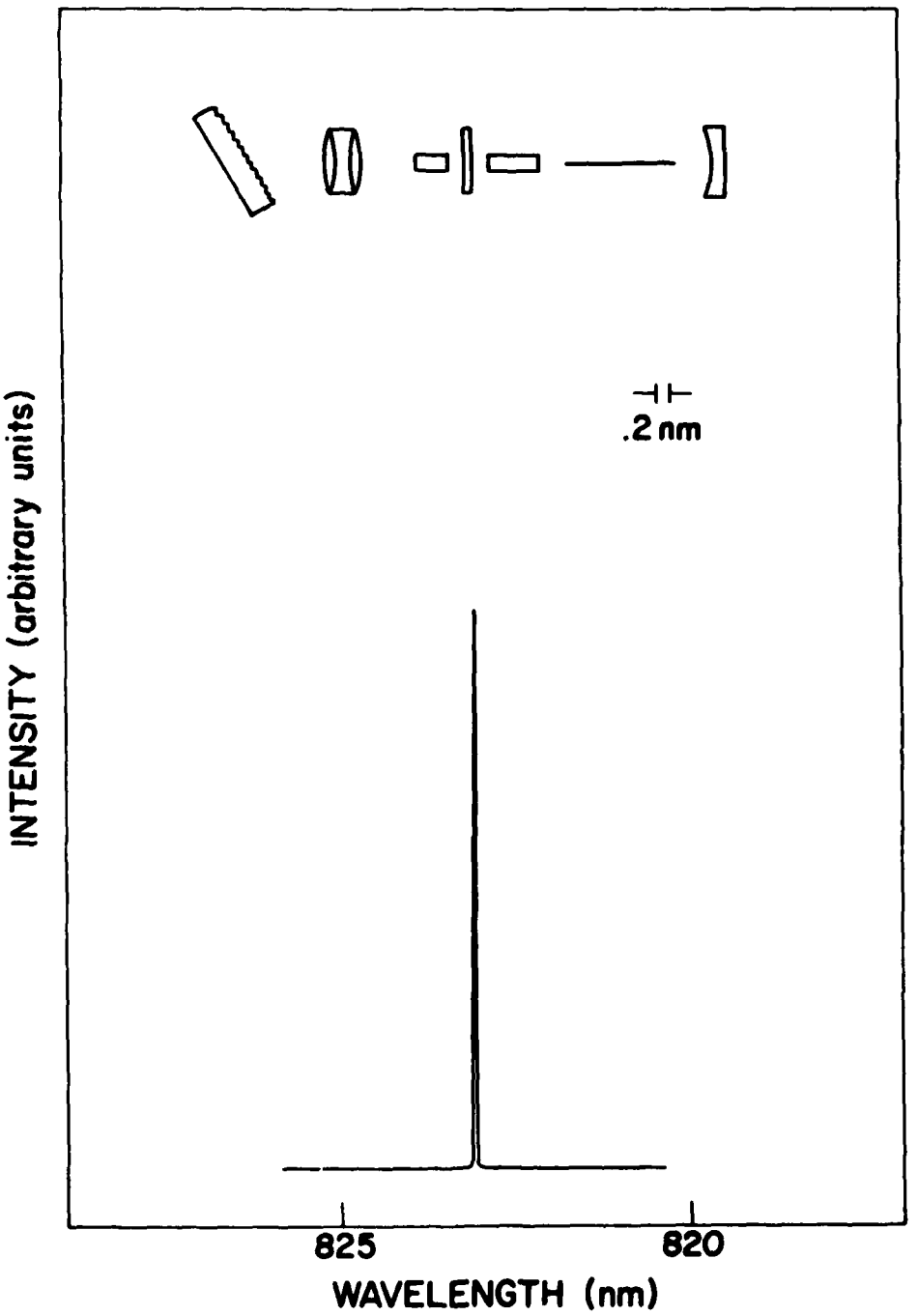

Figure 8

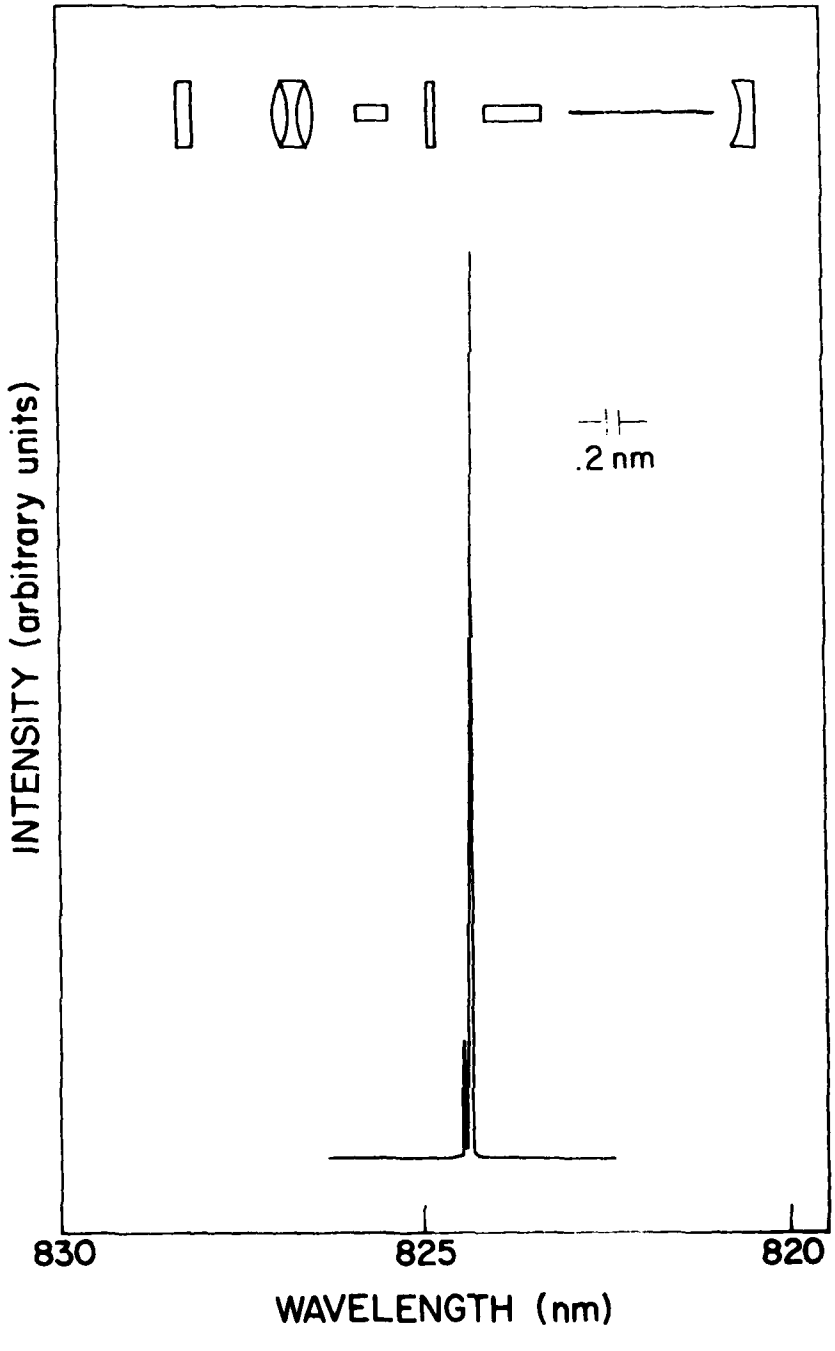

Figure 9

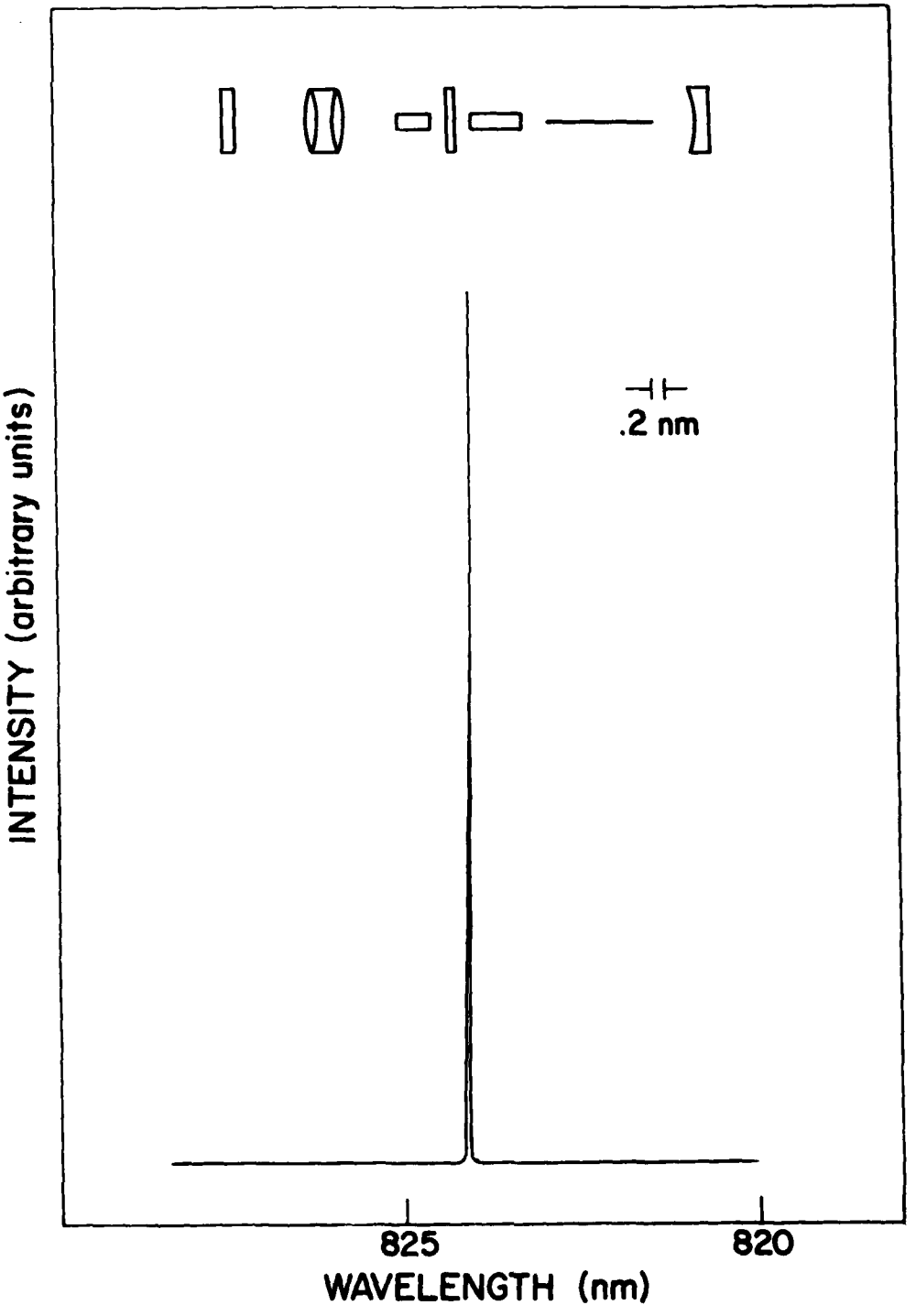

Figure 10a

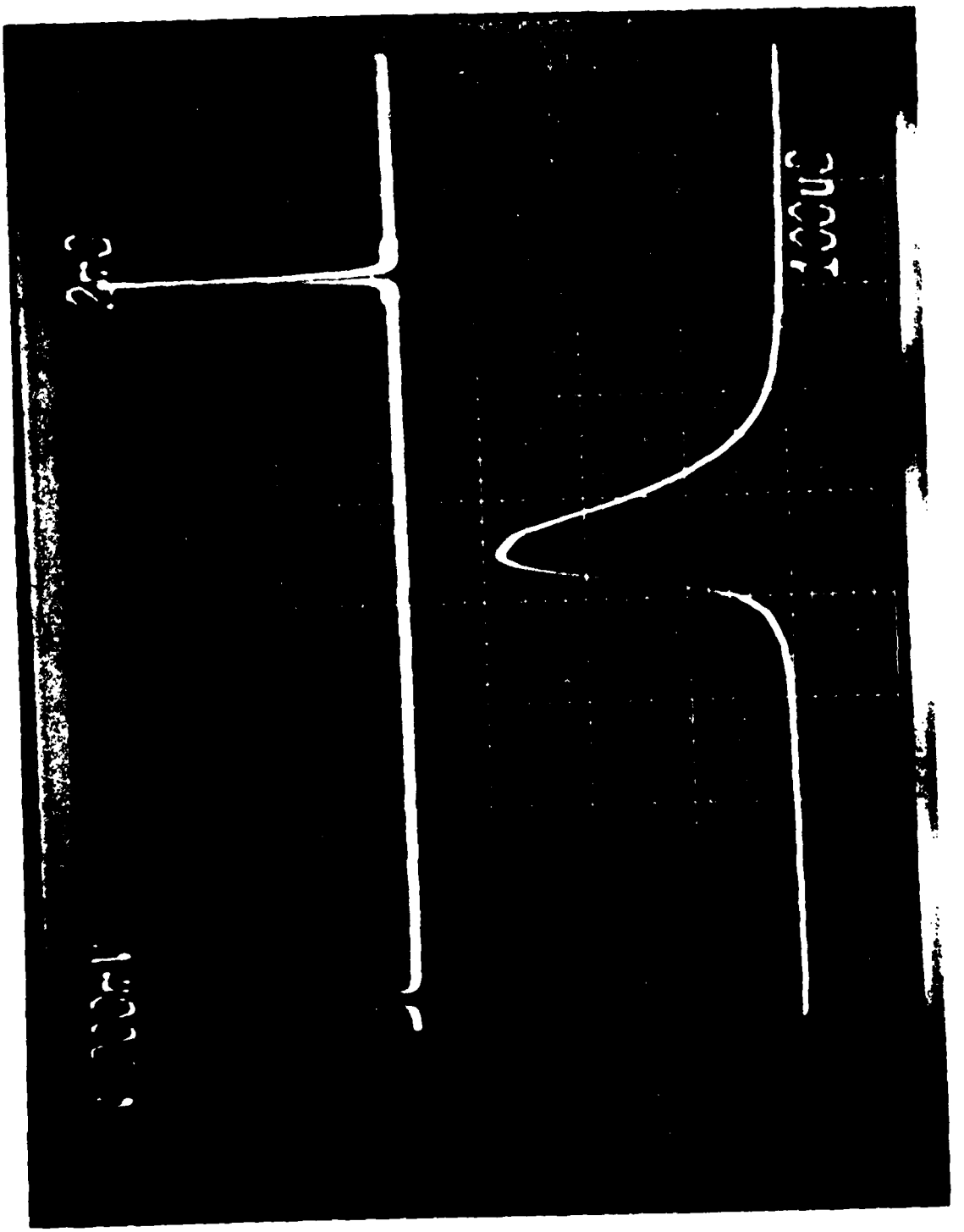

Figure 10b

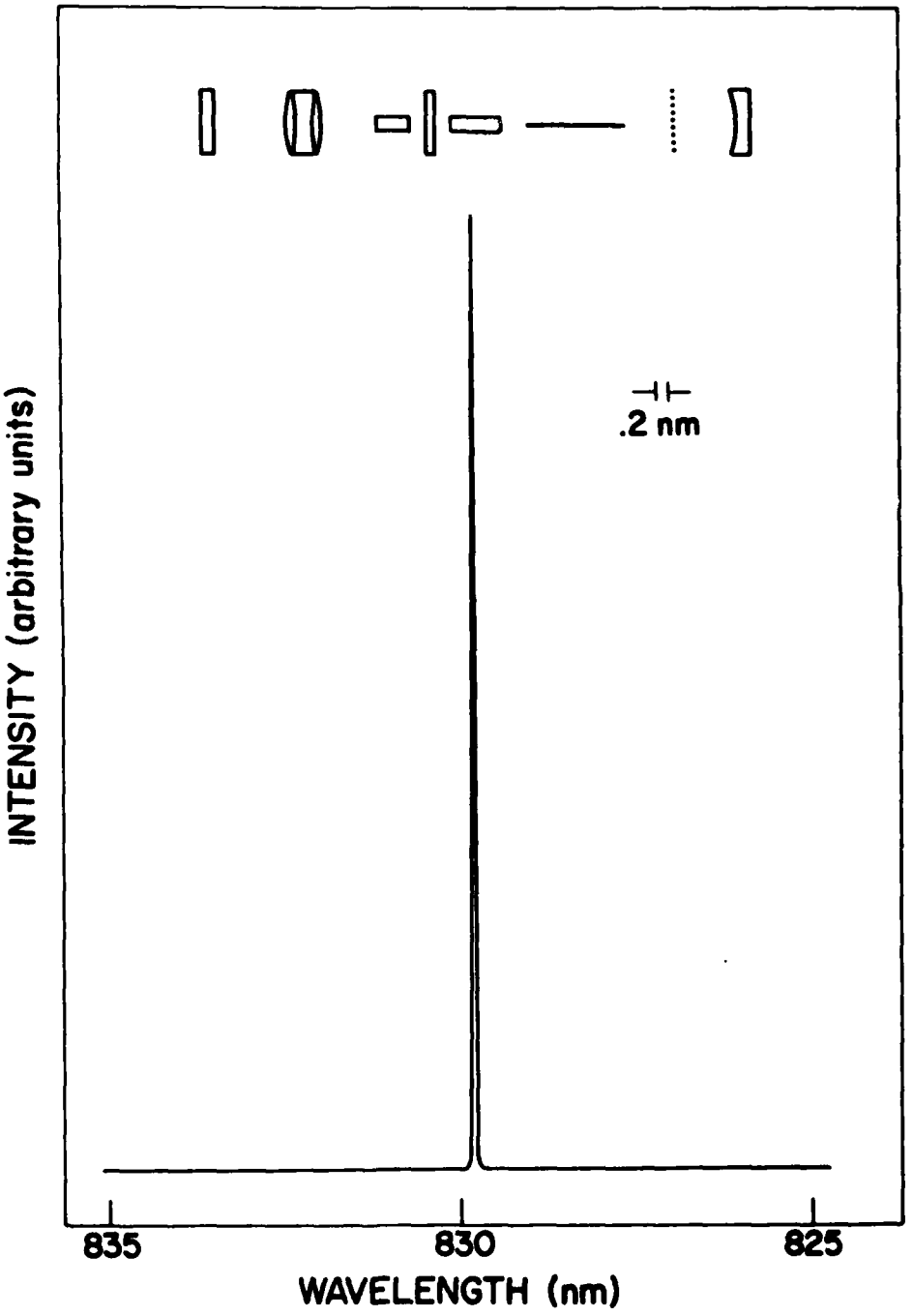

Figure 11a

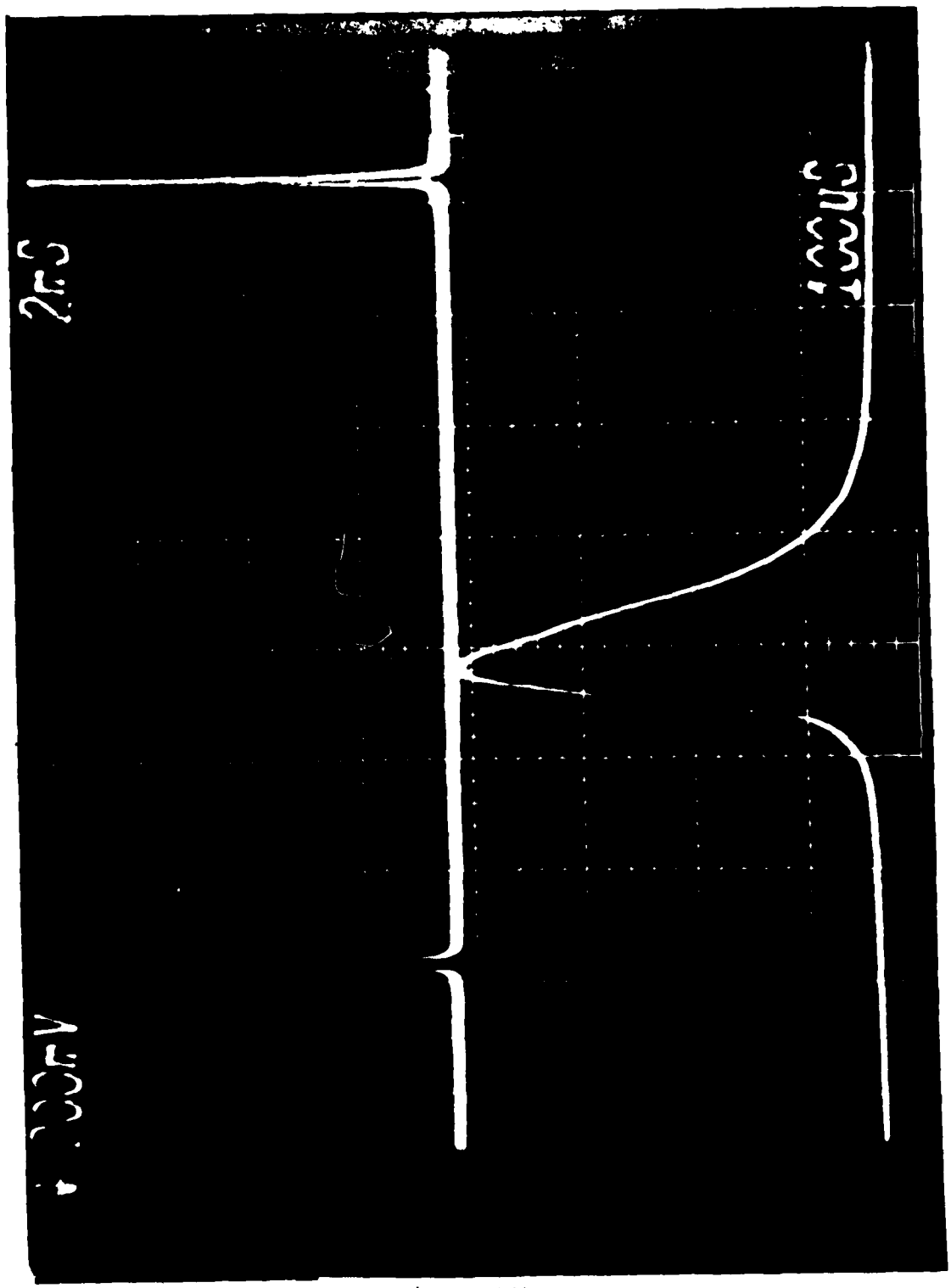

Figure 11b

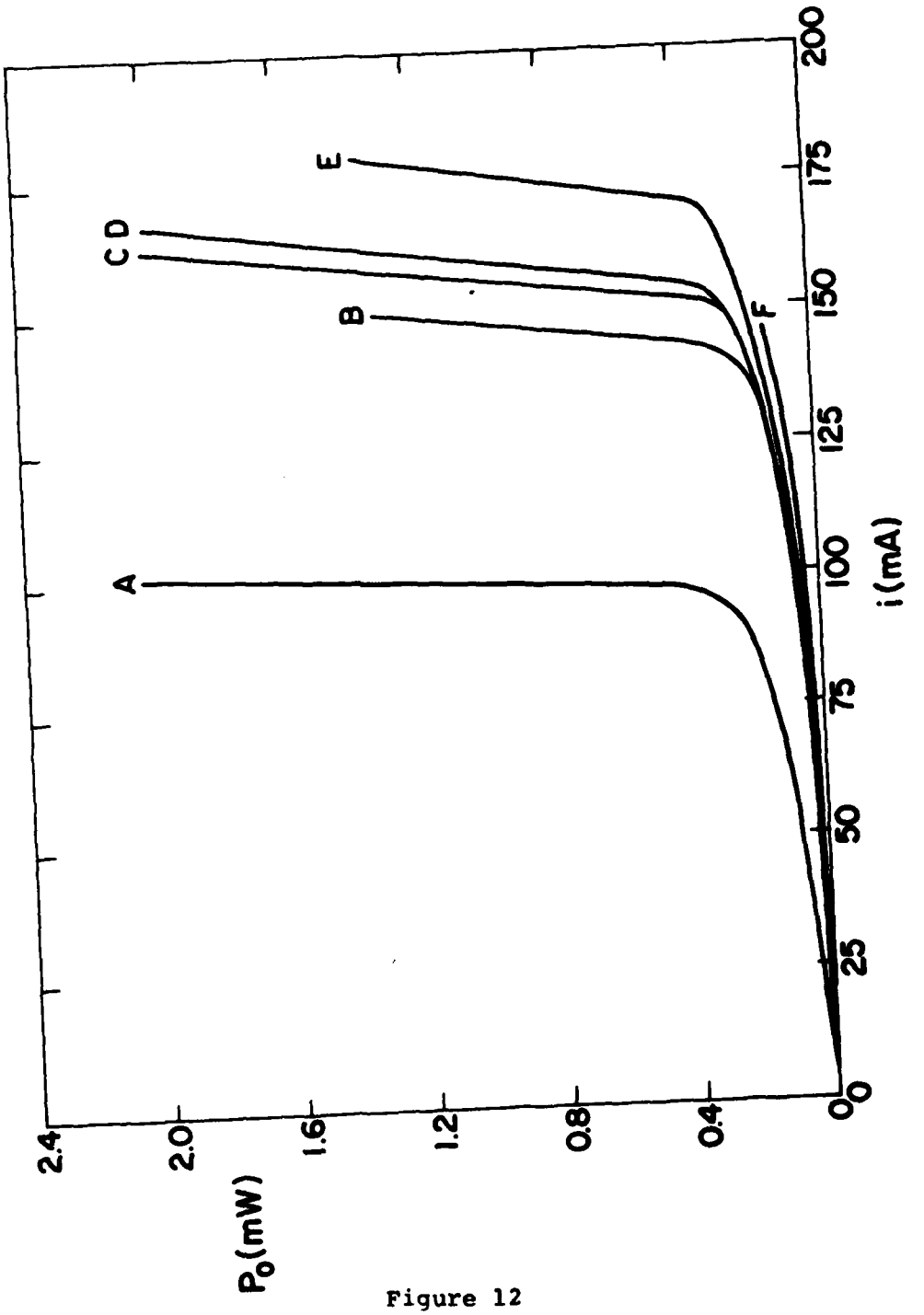

Figure 12

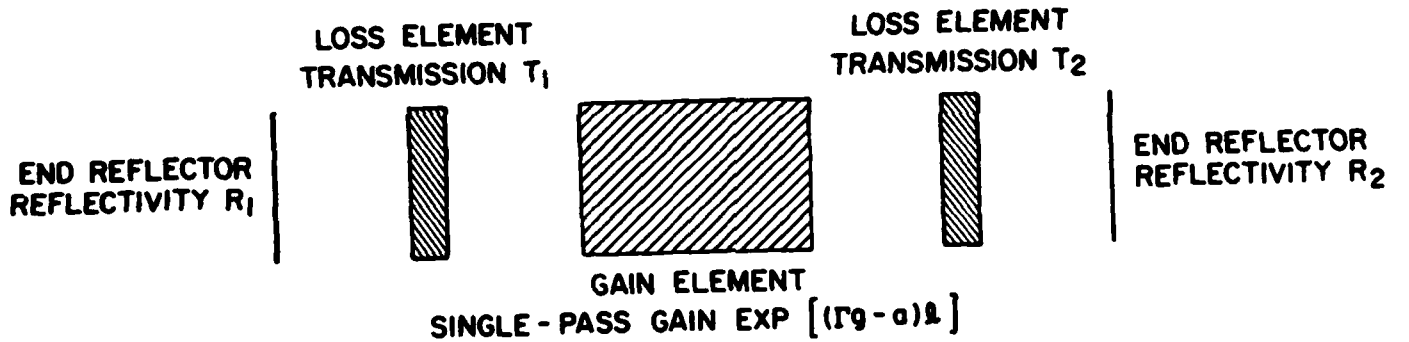
LOSS ELEMENT
TRANSMISSION T_1
LOSS ELEMENT
TRANSMISSION T_2
END REFLECTOR
REFLECTIVITY R_1
END REFLECTOR
REFLECTIVITY R_2
GAIN ELEMENT
SINGLE - PASS GAIN EXP $[(\Gamma g - \alpha)\ell]$

Figure 13

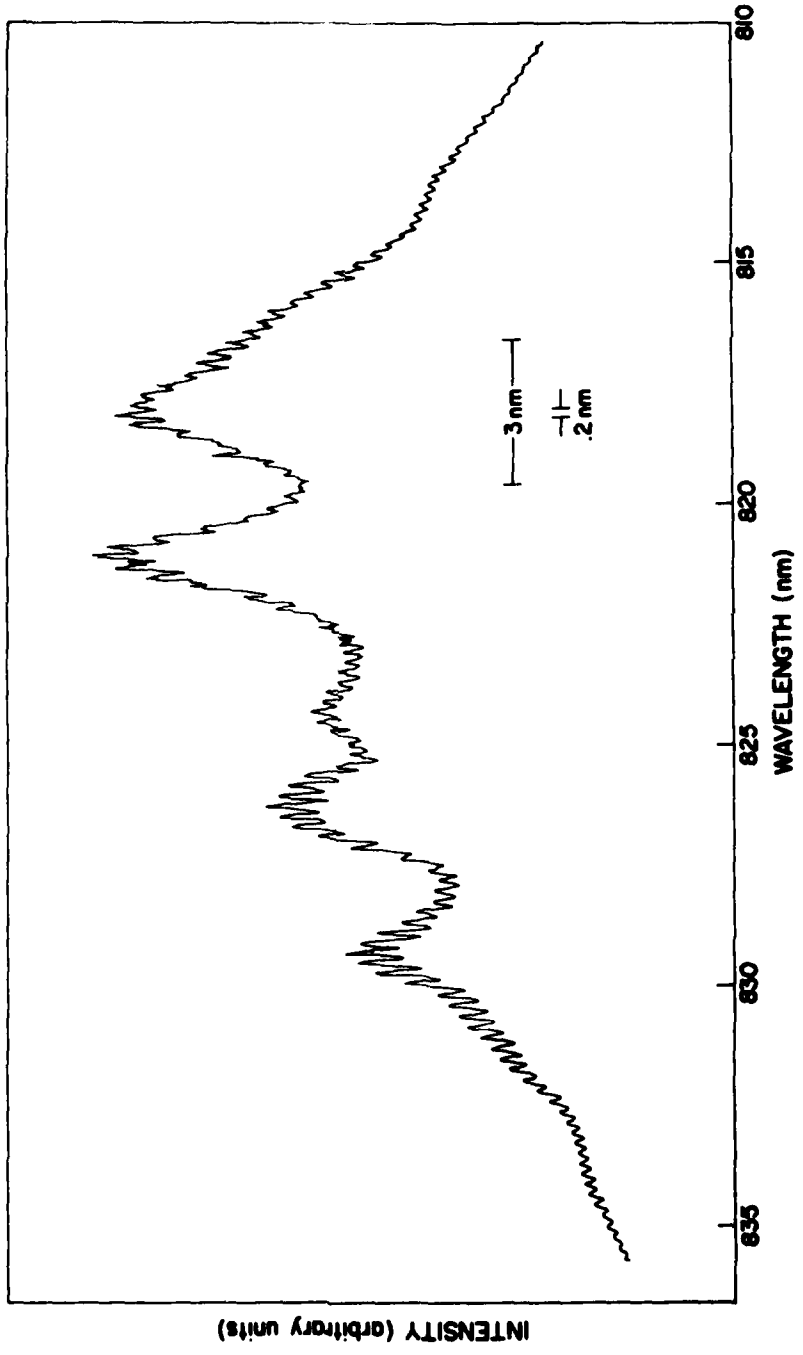
INTENSITY (arbitrary units)
WAVELENGTH (nm)
810
815
820
825
830
835
3nm
.2nm

Figure 14

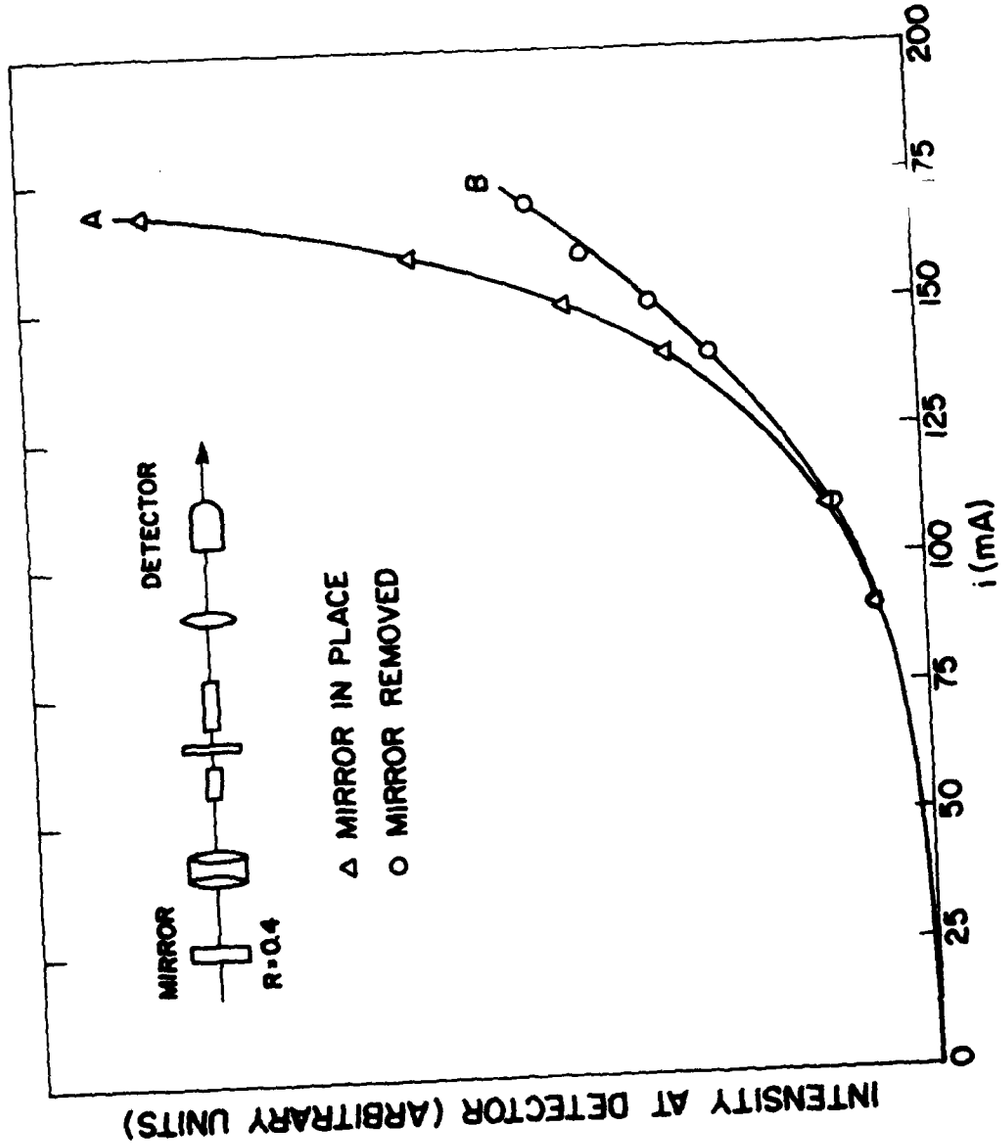
INTENSITY AT DETECTOR (ARBITRARY UNITS)
i (mA)
0
25
50
75
100
125
150
175
200
A
B
Δ MIRROR IN PLACE
O MIRROR REMOVED
DETECTOR
MIRROR
R=0.4

Figure A1

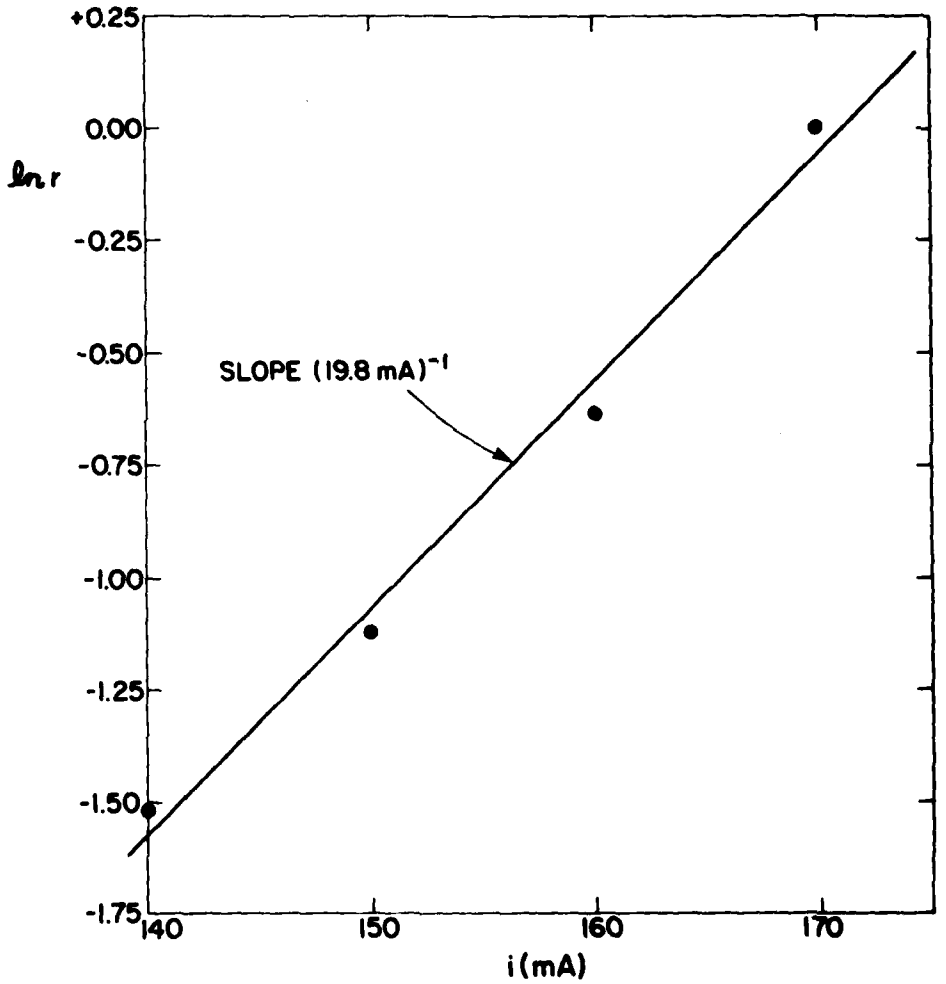
+0.25
0.00
-0.25
-0.50
-0.75
-1.00
-1.25
-1.50
-1.75
ln r
SLOPE (19.8 mA)$^{-1}$
140
150
160
170
i(mA)

Figure A2


DATE
ILME